



Title	Application of contrast-enhanced ultrasonography in diagnosis of canine pancreatic disease
Author(s)	Lim, Sue Yee
Citation	北海道大学. 博士(獣医学) 甲第11519号
Issue Date	2014-09-25
DOI	10.14943/doctoral.k11519
Doc URL	<a href="http://hdl.handle.net/2115/57316">http://hdl.handle.net/2115/57316</a>
Type	theses (doctoral)
File Information	Lim Sue Yee.pdf



[Instructions for use](#)

Application of contrast-enhanced ultrasonography  
in diagnosis of canine pancreatic disease

(犬の膵疾患の診断における  
造影超音波検査の応用)

**Lim Sue Yee**

## GENERAL ABBREVIATIONS

AP	Acute pancreatitis
AUC	Area under the curve
AUROC	Area under the ROC curve
CBC	Complete blood count
CCK	Cholecystokinin
CEUS	Contrast-enhanced ultrasonography
CrPDA	Cranial pancreaticoduodenal artery
CrPDV	Cranial pancreaticoduodenal vein
CT	Computed tomography
IV	Intravenous
LS	Least squares
MB	Microbubble
MI	Mechanical index
MPV	Mean pixel value
PI	Peak intensity
ROC	Receiver operating characteristic
ROI	Region of interest
TIC	Time-intensity curve
T <sub>p</sub>	Peak time
TTU	Time to initial up-slope
TTW	Time to wash-out
US	Ultrasound

# TABLE OF CONTENTS

<b>GENERAL INTRODUCTION.....</b>	<b>1</b>
----------------------------------	----------

## **CHAPTER 1**

### **QUALITATIVE AND QUANTITATIVE CONTRAST-ENHANCED**

### **ULTRASONOGRAPHY OF THE PANCREAS USING BOLUS INJECTION AND**

### **CONTINUOUS INFUSION METHODS IN NORMAL DOGS .....5**

1. INTRODUCTION .....	6
-----------------------	---

2. MATERIALS AND METHODS.....	7
-------------------------------	---

2.1 Animals .....	7
-------------------	---

2.2 Bolus injection and continuous infusion of contrast agent .....	7
---	---

2.3 B-mode US and CEUS.....	8
-----------------------------	---

2.4 Quantitative analysis .....	9
---------------------------------	---

2.5 Statistical Analysis.....	9
-------------------------------	---

3. RESULTS .....	11
------------------	----

3.1 CEUS findings .....	11
-------------------------	----

3.2 Statistical analysis .....	12
--------------------------------	----

4. DISCUSSION .....	19
---------------------	----

5. SUMMARY .....	23
------------------	----

## **CHAPTER 2**

### **QUALITATIVE AND QUANTITATIVE CONTRAST-ENHANCED**

### **ULTRASONOGRAPHIC ASSESSMENT OF CERULEIN-INDUCED ACUTE**

### **PANCREATITIS IN DOGS.....24**

1. INTRODUCTION .....	25
2. MATERIALS AND METHODS.....	27
2.1 Animals.....	27
2.2 Cerulein-induced acute pancreatitis.....	27
2.3 B-mode US and CEUS.....	27
2.4 Quantitative analysis.....	28
2.5 Statistical analysis.....	29
3. RESULTS .....	30
3.1 Cerulein-induced acute pancreatitis.....	30
3.2 US findings .....	30
3.3 CEUS findings .....	31
3.4 Statistical analysis.....	31
4. DISCUSSION.....	37
5. SUMMARY.....	41

### **CHAPTER 3**

#### **QUANTITATIVE CONTRAST-ENHANCED ULTRASONOGRAPHIC**

#### **ASSESSMENT OF NATURALLY OCCURRING PANCREATITIS IN DOGS .....42**

1. INTRODUCTION .....	43
2. MATERIALS AND METHODS.....	44
2.1. Patients.....	44
2.2 B-mode US and CEUS.....	44
2.3 Quantitative analysis.....	45
2.4 Statistical analysis.....	46
3. RESULTS .....	47

3.1 Animals .....	47
3.2 B-mode US.....	47
3.3 CEUS findings .....	47
3.4 Statistical analysis .....	49
4. DISCUSSION .....	56
5. SUMMARY .....	61
<b>GENERAL CONCLUSION.....</b>	<b>62</b>
<b>JAPANESE SUMMARY.....</b>	<b>65</b>
<b>REFERENCES.....</b>	<b>69</b>
<b>ACKNOWLEDGEMENTS .....</b>	<b>77</b>

## GENERAL INTRODUCTION

The canine pancreas consists of two components, the predominant exocrine portion and the small endocrine portion. Diseases of the exocrine pancreas are common in companion animals and pancreatitis is the most common exocrine disease seen in dogs.<sup>1</sup> Although a common consensus has not been reached for its classification, it can generally be divided into acute and chronic presentations.<sup>2,3</sup> There has been much confusion on the definition of classification of pancreatitis in veterinary medicine and this is because pathological classifications are dependent on histological descriptions. However, because different types of pancreatitis overlap in their clinical presentation and biopsy specimens are often not obtained, a clinical bias in terminology based on duration of clinical signs exists.<sup>2,3</sup> Clinical signs exhibited by dogs with either forms of pancreatitis are non pathognomonic for the disease.<sup>4,5</sup>

Currently, there is no single noninvasive diagnostic method that is completely reliable for the antemortem diagnosis of pancreatitis in dogs. One should take into account the complete history, physical examination findings, clinicopathologic results, measurement of pancreatic lipase immunoreactivity, radiography and ultrasound (US) examination of the pancreas for an accurate noninvasive diagnosis of pancreatitis.<sup>6</sup>

US is one of the most widely used imaging modalities, due to its characteristics such as real-time scanning, radiation free, operational ease, and cost-effectiveness. US findings in canine acute pancreatitis (AP) include an enlarged, irregular or mass-like pancreas with areas of patchy hypoechoic to mixed patterns of echogenicity. The surrounding mesentery may appear hyperechoic with the possible presence of focal abdominal fluid, corrugation of the neighboring duodenum, and ultrasonographic signs of extrahepatic bile duct obstruction.<sup>4,7</sup> A hyperechoic pancreas can be associated with chronic cases of pancreatitis due to the presence

of pancreatic fibrosis.<sup>8</sup> US is useful in the diagnosis of AP in dogs, but has a reported sensitivity of only 68% so an unremarkable US examination does not rule out pancreatitis.<sup>4,7</sup>

Contrast-enhanced ultrasonography (CEUS) is a major breakthrough for US imaging in recent years. CEUS utilizes microbubbles (MB) as contrast agent and contrast-specific imaging modalities for real time perfusion imaging of organs.<sup>9</sup> Sonazoid®, a second generation contrast agent, contains perfluorobutane gas of low solubility encapsulated by a lipid shell, and is highly stable *in vivo*.<sup>10</sup> These MB are entirely intravascular when administered intravenously, with no extravasation into surrounding tissue. When exposed to intermediate acoustic power ( $0.1 < \text{mechanical index (MI)} < 0.5$ ),<sup>9</sup> it develops nonlinear resonance, resulting in harmonic signals with minimal destruction, thus providing continuous real-time contrast imaging of longer duration.<sup>9</sup> Subtraction techniques such as pulse inversion imaging, used in contrast-specific imaging modalities, enhance detection of nonlinear resonance from MB with high sensitivity while suppressing echoes from tissues.<sup>9</sup> Therefore, the contrast-enhancement reflects perfusion of the organ. The typical perfusion pattern of an organ will differ according to different methods (e.g., bolus injection, slow bolus injection, or continuous infusion) of contrast agent administration.<sup>11</sup>

CEUS is used most extensively in human medicine for cardiac and liver imaging and has expanded to other abdominal organs such as the pancreas, kidney, spleen, thyroid, and prostate.<sup>12,13</sup> The application of CEUS in veterinary medicine is growing and is mainly used in the diagnosis of diseases of the liver, spleen, and kidney.<sup>14-19</sup> CEUS has been particularly useful in the differentiation of malignant neoplasia from benign nodules in the canine liver with high accuracy.<sup>14</sup> Other studies in normal dogs exist for the pancreas, duodenum, jejunum, adrenal glands, prostate, and lymph nodes.<sup>20-24</sup> Applications of CEUS in the diagnosis of pancreatic neoplasia have also been reported in veterinary medicine.<sup>25,26</sup>

In human medicine, contrast-enhancement of the pancreas is reported to be well correlated with its perfusion, and can differentiate areas of inflammation (hyperechoic enhancement) and necrosis (non-enhancement).<sup>27-30</sup> The main indications of CEUS in pancreatic diseases in people are AP, neoplasia, and pseudotumors.<sup>27,31,32</sup> CEUS has been reported to be comparable to computed tomography (CT) for assessment of AP in people.<sup>32,33</sup> These studies have showed the usefulness of CEUS in detection, staging severity, and predicting clinical outcomes of AP. However, studies in dogs with AP are few and to my knowledge only one report and one abstract exist to date.<sup>34,35</sup> The former describes the detection and characterization of focal hypovascular lesions within the pancreatic parenchyma of dogs with AP,<sup>34</sup> while the latter remains as an abstract describing perfusion changes of the pancreatic parenchyma in naturally occurring pancreatitis in a small number of dogs.<sup>35</sup>

*In vivo* animal models of AP are particularly useful as studies of pancreatitis in the clinical setting faces limitations. A variety of well-developed AP models exist. These models can be noninvasive or invasive, ranging from diet manipulations (e.g., choline-deficient ethionine supplement diet) to exogenous chemical administration (e.g., cerulein infusion) that are noninvasive, or even surgical manipulation-induced pancreatitis (e.g., common biliopancreatic duct ligation) that are invasive.<sup>36</sup>

With the above background, this study was performed in 3 stages to determine the feasibility of using quantitative CEUS in the diagnosis of canine pancreatic disease, in particular pancreatitis. In the first stage, I have characterized and compared contrast-enhancement of the normal canine pancreas using bolus injection and continuous infusion of MB contrast agent. The results from this stage established the baseline perfusion patterns of the normal canine pancreas. In the second stage, I have investigated feasibility of CEUS in detecting perfusion changes in the pancreas of dogs with experimentally induced pancreatitis.

CEUS proved to be useful in detecting perfusion changes in the inflamed pancreas. Using the results from this stage, I then proceeded in the third stage to investigate the feasibility of CEUS as a noninvasive diagnostic tool in naturally occurring canine pancreatitis by detecting these changes in pancreatic perfusion.

## **CHAPTER 1**

# **QUALITATIVE AND QUANTITATIVE CONTRAST-ENHANCED ULTRASONOGRAPHY OF THE PANCREAS USING BOLUS INJECTION AND CONTINUOUS INFUSION METHODS IN NORMAL DOGS**

## 1. INTRODUCTION

Detection and characterization of pancreatic diseases in human, such as AP, pancreatic adenocarcinoma and insulinoma, can be improved with CEUS.<sup>31,32,37</sup> Intravenous (IV) bolus injection of MB is the method most commonly employed for abdominal CEUS.<sup>14,18-20,38</sup> The typical time-intensity curve (TIC) for the pancreas following bolus injection shows a rapid increase followed by a short peak of strong enhancement with fast wash-out.<sup>20,27</sup> This pattern of enhancement means that the duration of diagnostically useful enhancement is brief, and repeat bolus injections may be required resulting in several short, interrupted periods of enhancement.

The canine pancreas is V-shaped and consists of two lobes, emerging from the body.<sup>39</sup> Due to its anatomy, the canine pancreas cannot be viewed entirely in a single US view.<sup>40</sup> These considerations allow us to foresee the difficulties in continuous imaging of multiple pancreatic regions with bolus injection method. The rapidity of enhancement may also result in perfusion parameter changes that are too minute (e.g. millisecond) to be detected. A continuous infusion method using an infusion pump may overcome the time limitation faced with bolus injection. It has been demonstrated that not only the duration of enhancement can be greatly prolonged, but also a constant plateau of enhancement throughout the duration of the infusion can be achieved with continuous infusion.<sup>41-43</sup>

Thus, the goal of chapter 1 was to (1) characterize image enhancement of the normal canine pancreas with duodenum as reference using bolus injection and continuous infusion with contrast agent Sonazoid® and to (2) assess if continuous infusion method can prolong the duration of pancreatic enhancement over that with bolus injection.

## **2. MATERIALS AND METHODS**

### **2.1 Animals**

Eight mixed-breed adult dogs, 1- 6 years old and weighing 11- 18 kg were studied. The dogs were healthy based on physical examination and exhibited no clinical signs or biochemical laboratory abnormalities (including lipase and C-reactive protein) suggesting pancreatic disease. Prior to CEUS studies, fundamental B-mode US was performed on the pancreas and duodenum of each dog, and no evidence of focal or diffused abnormalities was observed. All procedures were approved by the Hokkaido University Animal Care and Use Committee.

### **2.2 Bolus injection and continuous infusion of contrast agent**

#### **2.2.1 Dosage**

Sonazoid<sup>®</sup> (Daiichi-Sankyo, Tokyo, Japan) was the contrast agent used for this experiment. For bolus injection, I have estimated that a MB contrast agent dose of 0.01 mL/kg would be suitable based on manufacturer's recommendation (0.015 mL/kg) and clinical experiences with canine liver and spleen imaging in our facility.<sup>14,16,38</sup> For continuous infusion of MB contrast agent, based on preliminary studies, a dose 5 times of the bolus injection dose (0.05 mL/kg) that was reported to be safe was used.<sup>44</sup> Bolus injection and continuous infusion experiments were carried out on separate days for each dog, in order to eliminate residual effects of MB contrast agent in the organs of interest or blood circulation.

#### **2.2.2 Technique**

For bolus injection, a single bolus of contrast agent was administered by hand through a 21 G butterfly catheter attached to a 22 G IV catheter placed in the cephalic vein, flushed

by 3 mL of heparinized saline. For continuous infusion model, a single infusion of contrast agent diluted to 5 mL of saline was administered using a syringe pump (Top-5300; Top, Tokyo, Japan ) at a rate of 5 mL/min. The contrast agent was diluted and gently shaken immediately before infusion. The injections were given in a standardized manner by the same person throughout the study. The timer on the US machine was manually started when the milky-white contrast agent entered the IV catheter.

## **2.3 B-mode US and CEUS**

### **2.3.1 Settings**

An US scanner (Aplio XG; Toshiba Medical Systems, Tochigi, Japan) with a 7-14 MHz broadband linear probe (PLT-1204 AT; Toshiba Medical Systems, Tochigi, Japan) was used for B-mode ultrasonography. A 5-11 MHz broadband linear probe (PLT-704 AT; Toshiba Medical Systems, Tochigi, Japan) suitable for pulse subtracting imaging was used for CEUS. Adjustable parameters were optimized during preliminary studies and maintained for all imaged dogs. MI was set at 0.21 to minimize MB destruction. Focus depth was placed below the pancreas. The B-mode and contrast imaging gain were set at 100 dB and 75 dB, respectively. US imaging was set at 30-31 frames/s, and the images were recorded in 40-second cine-loops to a hard disk for off-line analysis. Perfusion of the pancreatic parenchyma and duodenal mucosa was evaluated after IV bolus injection and continuous infusion of MB contrast agent.

### **2.3.2 Scanning**

Scanning was performed without sedation to exclude anesthetic influence on CEUS. The animal was positioned on left lateral recumbency, and the US probe was placed longitudinally between 2 ribs to image the transverse view of the right pancreatic lobe and

adjacent descending duodenum. Scanning was done continuously for 5 min after bolus injection and at the start of continuous infusion of MB contrast agent.

#### **2.4 Quantitative analysis**

US images were analyzed using an off-line image analysis (ImageJ; US National Institutes of Health, Bethesda, MD, U.S.A. ). In this system, the gray-scale level ranged from 0 to 255 mean pixel value (MPV). For bolus injection, one image per second for the first 60 seconds was analyzed. For continuous infusion, one image per second for the first 120 seconds followed by 1 image at an interval of every 10 seconds until 300 seconds from start of MB infusion was analyzed. Tissue intensity was measured for each of the region of interest (ROI), typically containing 300-600 pixels,<sup>19</sup> placed in the pancreatic parenchyma and duodenal mucosa for bolus injection and continuous infusion (Fig. 1D). When respiratory motion was present, the ROI was manually adjusted to maintain the same position within the pancreas and duodenum. A TIC was created for each injection model. The wash-in was reflected by time to initial up-slope (TTU) and peak time (Tp); peak intensity (PI) and the wash-out as reflected by time to wash-out (TTW) were measured in all ROIs (Fig. 2). TTU and TTW were defined as the time when the gray-scale level increased to and decreased to 30% of PI. All data were expressed as median and range.

#### **2.5 Statistical Analysis**

Normality of the data was tested using the Shapiro Wilk test. Because the data were not normally distributed, the Wilcoxon signed rank test was used to test for differences between pancreas and duodenum during bolus injection and continuous infusion, between pancreas during bolus injection and continuous infusion and between duodenum during bolus injection and continuous infusion for the four measured parameters. For all analyses, *P*-

values of  $< 0.05$  were considered statistically significant. Statistical analyses were performed with a statistical analysis program (JMP 8; SAS Institute Inc., Cary, NC, U.S.A.).

## 3. RESULTS

### **3.1 CEUS findings**

Pancreatic images from all eight dogs were included for analysis after bolus injection and continuous infusion. Images of the duodenum from one dog were excluded from the continuous infusion group due to inability to image both organs simultaneously in one field throughout the imaging period of 5 minutes. No adverse effects, such as dyspnea or anaphylaxis were noticed in any dogs during or after bolus injection or continuous infusion of MB contrast agent.

#### **3.1.1 Bolus injection**

Before contrast agent administration, the baseline tissue echo components of the pancreatic parenchyma and duodenal mucosa were minimal in the pulse subtraction CEUS mode. Some echogenic components were observed due to fat and gastrointestinal gas (Fig. 1A). After bolus injection, the cranial pancreaticoduodenal artery (CrPDA) was enhanced earliest (Fig. 1C). Soon after, enhancement of the pancreatic parenchyma was seen followed almost simultaneously by the duodenal mucosa (Fig. 3). The pancreatic parenchyma reached an intense peak several seconds later, slightly before or at the same time as the duodenal mucosa. The pancreas was more enhanced than the duodenum and was clearly delineated in the CEUS mode (Fig. 1D). Contrast effect of the pancreas and duodenum decreased sharply followed by a gradual loss of enhancement (Fig. 1E). The cranial pancreaticoduodenal vein (CrPDV) could still be seen at this time. Subjectively, the parenchyma of the pancreas and duodenum cannot be seen clearly when the intensity dropped to around 30 MPV.

### **3.1.2 Continuous infusion**

The continuous infusion method produced a different enhancement profile (Fig. 4) when compared to bolus injection. Initial enhancement of the CrPDA and pancreatic parenchyma was delayed compared to bolus injection. Initial enhancement of the duodenal mucosa was slightly slower compared to the pancreatic parenchyma. Image enhancement of the pancreatic parenchyma and duodenal mucosa was more gradual until its peak enhancement (Fig. 5A); thereafter, the pancreas was continuously enhanced (Fig. 5B). This period of enhancement lasted longer than the period of contrast agent infusion (1 min). Subjectively, the enhancement of the pancreas and duodenum was similar at PI, but was less homogeneously enhanced when compared to bolus injection. Thereafter, a gradual loss of enhancement was observed (Fig. 5C).

### **3.2 Statistical analysis**

The measured parameters for bolus injection and continuous infusion are summarized (Table 1). Median (range) contrast enhancement durations (TTW – TTU) of the pancreas and duodenum were prolonged by continuous infusion from 11 (10 to 23) s and 16 (3 to 43) s at bolus injection to 205 (170 to 264,  $P < 0.01$ ) s and 193 (169 to 216,  $P < 0.05$ ) s, respectively. Median (range) PI of the pancreas at bolus injection [100.9 (80.2 to 124.3) MPV] was significantly greater than median PI of the duodenum at bolus injection [86.5 (36.6 to 120.2) MPV;  $P < 0.01$ ] and median PI of the pancreas at continuous infusion [77.6 (58.2 to 99.5) MPV;  $P < 0.05$ ]. Contrast-enhancement of the pancreatic parenchyma was subjectively adequate with continuous infusion (Fig. 5A-C).

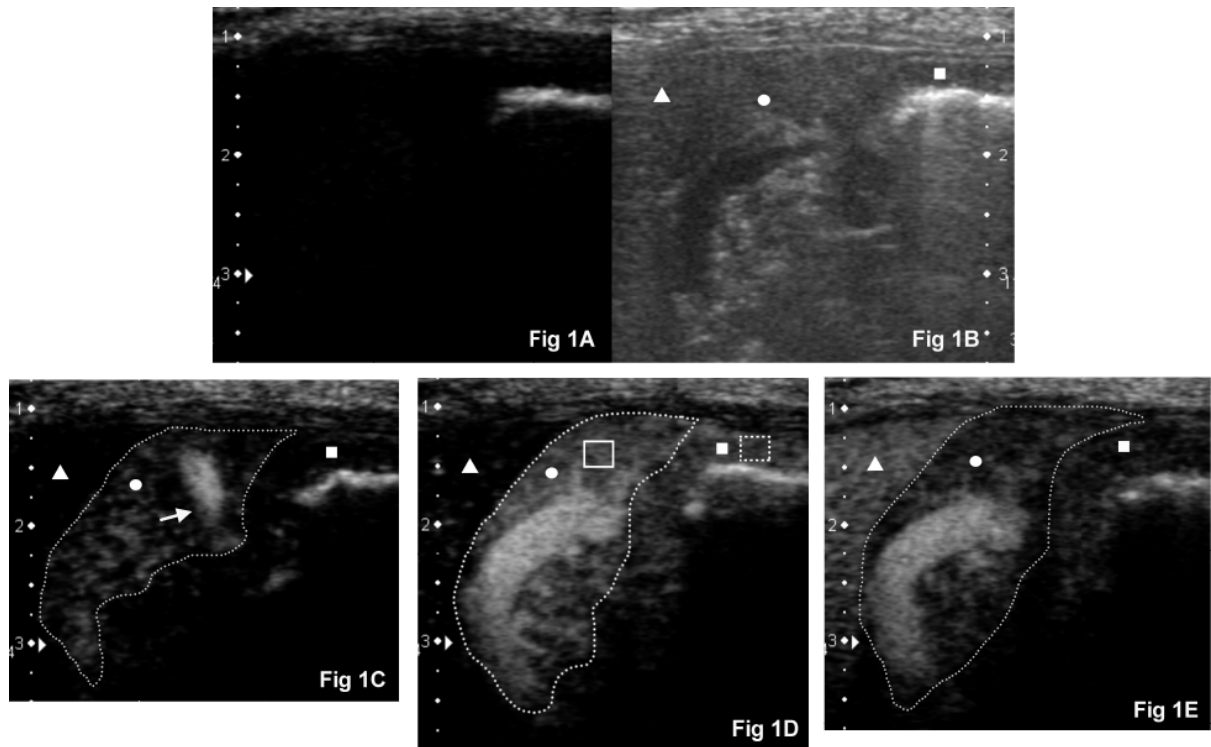


Figure 1. CEUS images of the pancreas and duodenum before and after bolus injection. Transverse view of the right pancreatic lobe (circle, outlined by a dotted line) and proximal descending duodenal mucosa (square) using the right intercostal approach imaging in a representative normal adult dog (dorsal is to the left, ventral is to the right, medial is to the bottom, and scales in cm to the left). (A) CEUS at 0 s. Baseline tissue echo components of the pancreatic parenchyma and duodenal mucosa were minimal in the CEUS mode. (B) Corresponding twin view B-mode image of (A). (C) CrPDA (white arrow) was more enhanced compared to the pancreatic parenchyma at 8 s after bolus injection of contrast agent. Duodenal mucosa was still unenhanced. (D) Both the pancreatic parenchyma and duodenum reached PI (shown here 12 s after bolus injection of contrast agent). The pancreas is well delineated from the non-enhancing neighboring liver (triangle). ROIs are manually placed in the pancreatic parenchyma (solid box) and duodenal mucosa (dashed box) to measure the tissue intensity. (E) Contrast washed out of the pancreatic parenchyma and duodenal mucosa at 20 s.

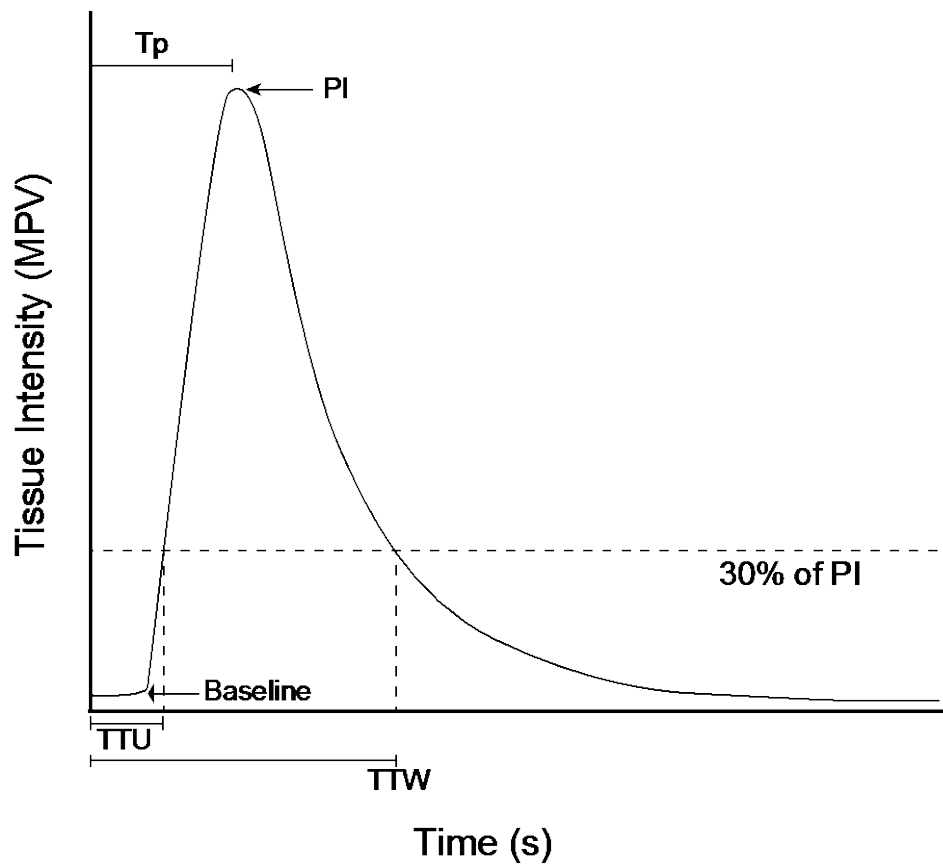


Figure 2. Representative TIC showing measured parameters. Baseline intensity remained unchanged until time to initial up-slope (TTU) when intensity first reached 30% of peak intensity (PI). Peak time ( $T_p$ ) was the time measured from contrast injection to PI. Time to wash-out (TTW) was measured from contrast injection to when intensity dropped to 30% of PI.

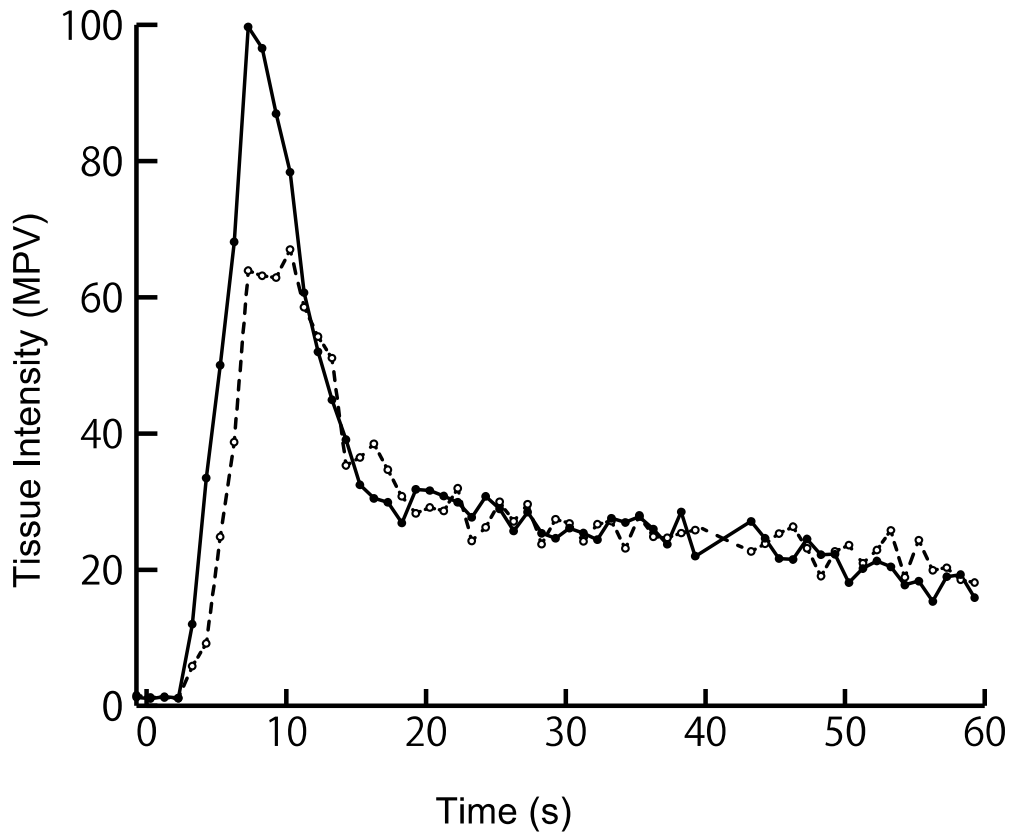


Figure 3. TIC showing the tissue intensity of the pancreatic parenchyma (solid line, ●, n = 8) and duodenal mucosa (dashed line, ○, n = 8) for 60 s after bolus injection of contrast agent. Notice the fast wash-in to sharp peak, followed by fast and then gradual decline in tissue intensity. Note that the x-axis is for 60 s. MPV= Mean pixel value.

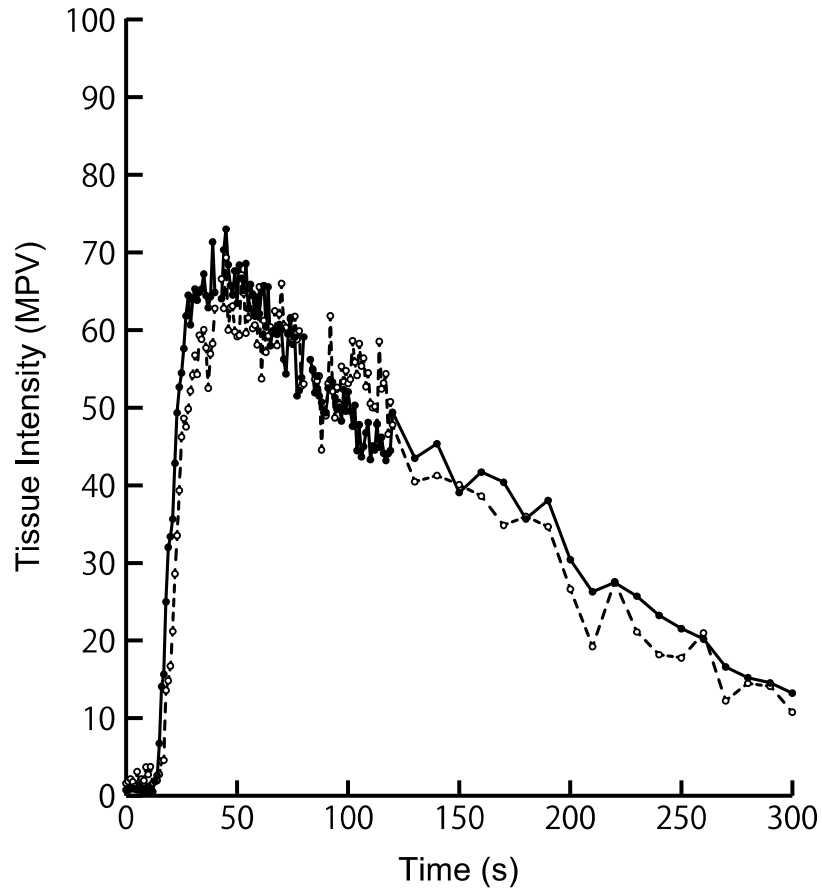


Figure 4. TIC showing the tissue intensity of the pancreatic parenchyma (solid line, ●, n = 8) and duodenal mucosa (dashed line, ○, n = 7) for 300 s after continuous infusion of contrast agent. Notice a more gradual wash-in to peak followed by a long plateau and slow wash-out of tissue intensity when compared with that of bolus injection in figure 3. Note that the x-axis is for 300 s. MPV= Mean pixel value.

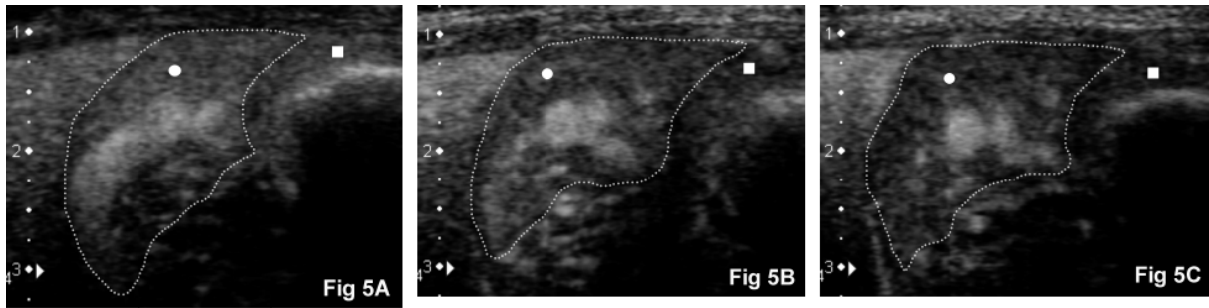


Figure 5. CEUS images of the pancreas and duodenum after continuous infusion of contrast agent. Right pancreatic lobe (circle, outlined by a dotted line) and duodenal mucosa (square) in the same representative adult dog as figure 1 (dorsal is to the left, ventral is to the right, medial is to the bottom, and scales in cm to the left). (A) PI of the pancreatic parenchyma at 43 s. (B) Contrast enhancement of the pancreatic parenchyma persisted at 108 s with (C) gradual wash-out as seen here at 172 s.

Table 1. Results (median, range) of the measured parameters of the TIC measured after bolus injection and continuous infusion in the normal pancreas and duodenum of healthy dogs.

Measured parameters	Bolus injection		Continuous infusion	
	Pancreas	Duodenum	Pancreas	Duodenum
TTU (s)	6.0 (4.0- 8.0)	7.5 (4.0- 9.0)	20.0 (16.0- 25.0) <sup>b,c</sup>	22.0 (18.0- 26.0) <sup>d</sup>
Tp (s)	8.5 (8.0- 10.0)	10.5 (6.0- 12.0)	33.0 (19.0- 52.0) <sup>c</sup>	52.0 (25.0- 66.0) <sup>d</sup>
TTW (s)	17.0 (15.0- 30.0)	23.5 (10.0- 49.0)	225.0 (190.0- 280.0) <sup>c</sup>	215.0 (169.0- 216.0) <sup>d</sup>
PI (MPV)	100.9 (80.2- 124.3) <sup>a</sup>	86.5 (36.6- 120.2)	77.6 (58.2- 99.5) <sup>d</sup>	70.2 (60.9- 90.3)

TTU, Time to initial up-slope; Tp, Peak time; TTW, Time to wash-out; PI, Peak intensity; MPV, Mean pixel value.

<sup>a</sup>Significant ( $P < 0.01$ ) difference versus duodenum during bolus injection.

<sup>b</sup>Significant ( $P < 0.05$ ) difference versus duodenum during continuous infusion.

<sup>c</sup>Significant ( $P < 0.01$ ) difference versus bolus injection for corresponding organ.

<sup>d</sup>Significant ( $P < 0.05$ ) difference versus bolus injection for corresponding organ.

## 4. DISCUSSION

In this study, after MB contrast agent administration as bolus or continuous infusion, the pancreas was clearly delineated from surrounding organs enabling good visualization. TTU, Tp, and TTW of the pancreas and duodenum were significantly prolonged with continuous infusion when compared to bolus injection. The enhancement duration of the pancreas and duodenum was also significantly prolonged with continuous infusion. Although PI of the pancreas was decreased significantly with continuous infusion, the pancreas was still adequately enhanced.

For bolus injection, the pancreas and duodenum had a similar early, intense, and uniform enhancement, as could be expected in organs receiving all its blood and therefore MB directly from the arterial supply.<sup>27</sup> The enhancement was followed by a sharp peak and then a fast initial decline; followed by a gradual washout. The patterns of enhancement of these organs were similar to another study on the canine pancreas and duodenum.<sup>20</sup> For continuous infusion, the enhancement of the pancreas and duodenum was initially delayed and was more gradual until it reached its peak and then plateaued. This was followed by a slow wash-out. The order at which pancreas and duodenum were enhanced did not change with bolus injection or continuous infusion.

Measured parameters TTU, Tp, and TTW were significantly prolonged in the pancreas and duodenum using continuous infusion method when compared to bolus injection. This result can be expected, because in continuous infusion, MBs were infused steadily and continuously over a minute in comparison to the quick bolus injection. Reasonably, it took a longer time for the enhancement of the pancreas and duodenum to be appreciable visually, thus a longer TTU and Tp. The contrast enhancement was prolonged, because of the

continuous inflow of MB into the ROI leading to slow wash-out as shown by prolonged TTW. This effect was beneficial, because the duration of diagnostically useful enhancement for the pancreas and duodenum was prolonged to 18 and 12 times, respectively when compared to bolus injection, even though the continuous infusion dose used was only 5 times the bolus injection dose.

Tp of the duodenum was later than the pancreas in continuous infusion, but not in bolus injection. This could be explained by the vascular supply of these organs. The pancreatic blood supply originates from the celiac artery through the splenic and hepatic arteries. The splenic artery is the primary blood supply to the left lobe of the pancreas. The hepatic artery terminates as the CrPDA, which enters the body of the pancreas and courses through the proximal portion of the right lobe of the pancreas. Branches from the CrPDA exit the pancreatic tissue and supply the closely associated duodenum.<sup>45</sup> In bolus injection, this order of vascular supply was not appreciable because of the fast speed of MB washing in. However, because buildup of MB to PI was slower in continuous infusion, the order of this vascular supply became appreciable, although not statistically significant.

The pancreatic parenchyma was less homogeneously enhanced during continuous infusion when compared to bolus injection. This could be explained by the lesser amount of MB at PI due to diluted MB during continuous infusion. This is in contrast to bolus injection where all MB injected perfused the ROI almost simultaneously in high concentration. Lower PI was significantly evident in the pancreas; however, imaging of the pancreas was visually adequate. Using continuous infusion, a reduction of 23% in the PI of the pancreatic parenchyma was comparable to 16% reduction in a previous continuous infusion CEUS study of the liver in which enhancement was deemed adequate despite that reduction.<sup>43</sup>

The obvious advantage of bolus injection is that it is easy to administer, less cumbersome, more repeatable, gives good tissue to tumor contrast, and is the conventional

method employed in characterizing nodular lesions.<sup>12,14-17,46-48</sup> However, contrast-enhancement is too rapid and brief in the pancreas.<sup>27</sup> These limitations were also seen in the present study with bolus injection as the pancreas and duodenum were enhanced rapidly and briefly.

Continuous infusion method provides a gradual increase in tissue intensity and longer period of tissue enhancement,<sup>43</sup> however, necessitating a higher dose in this study to achieve adequate imaging. Extra equipment (e.g. syringe pump) and personnel were also needed. The continuous infusion method may therefore be potentially useful in detecting differences in pancreatic perfusion in diffuse pancreatic disease that may otherwise be too subtle for detection using bolus injection method. The prolonged enhancement of the pancreas may also allow screening of the pancreas for hypovascular areas, such as necrosis. For other applications, such as characterization of nodular lesions, bolus injection should be applied so that the lesion can be studied dynamically in comparison with surrounding normal parenchyma. However, because no lesions were included into this study, further research is needed to determine when the bolus or continuous infusion method is preferable.

TTU can be taken as the time from contrast agent injection to when a certain percentage of increase in baseline tissue intensity is observed.<sup>20</sup> However, as the baseline tissue intensity was set to a minimum (nearing zero) in this study, this method was not feasible. Another method of determining wash-in time is when tissue intensity reaches a certain percentage of PI.<sup>31</sup> In this study, TTU and TTW were defined as time when the gray-scale level increased and decreased to 30% of PI. This percentage resulted in tissue intensity values of above 20 MPV for both bolus and continuous infusion methods. In the gray-scale, an increase of more than 20 units is generally needed for visual recognition.<sup>48</sup>

Previous CEUS studies performed in veterinary medicine employed the usage of sedatives or general anesthesia.<sup>19-21</sup> In the present study, no sedatives were used to eliminate

its confounding effects on patterns of contrast-enhancement. However, without sedatives, imaging was affected by greater motion and respiratory artifact. These movements can affect the TIC, because of difficulties in maintaining a similar ROI throughout the entire imaging period. Other than that, because of the placement of US probe parallel to the ribs, excessive movements might cause acoustic shadowing effects from the ribs resulting in compromised images with lowered tissue intensity, or which cannot be analyzed. Therefore, great care was taken to place ROIs manually at similar locations whenever possible while avoiding large blood vessels. Applying these precautions resulted in a more homogeneous TIC.

However, large variation was seen in PI both in bolus injection and continuous infusion. Looking at individual data, all dogs had higher PI in pancreas compared to duodenum, except for one dog receiving continuous infusion. The different PI could be attributed to individual differences and perfusion status of an individual animal at any one time. Therefore, the duodenum could be used as an internal control when investigating CEUS pattern of the pancreas. However, it is important to remember that diseases of the pancreas, such as pancreatitis may affect the surrounding organs including the duodenum.<sup>49</sup>

In conclusion, CEUS using bolus injection and continuous infusion methods can be used in dogs to image the pancreas. However, bolus injection results in rapid enhancement with fast wash-out and only provides a brief window for pancreatic imaging. On the other hand, continuous infusion provides gradual and prolonged enhancement that may be more useful in detecting tissue perfusional changes. With these findings, chapter 2 will be studied using the continuous infusion method to detect perfusion changes in the pancreas and duodenum in dogs with experimentally induced pancreatitis.

## 5. SUMMARY

In this chapter, I have characterized contrast-enhancement of the normal pancreas, and compared two methods of contrast agent administration to assess if continuous infusion of MB can prolong the duration of pancreatic enhancement over bolus injections. Fast wash-in to intense peak, followed by rapid wash-out was observed for TIC of bolus injection. With continuous infusion, contrast wash-in to PI was gradual, followed by long plateau and slow wash-out. Median contrast-enhancement durations of the pancreas and duodenum were significantly prolonged by continuous infusion. However, median PI of the pancreas was lower in continuous infusion when compared to bolus injection. Prolonged continuous imaging was afforded by continuous infusion of contrast agent. PI of the pancreas was slightly diminished in continuous infusion, but offered adequate imaging subjectively.

## **CHAPTER 2**

# **QUALITATIVE AND QUANTITATIVE CONTRAST-ENHANCED ULTRASONOGRAPHIC ASSESSMENT OF CERULEIN-INDUCED ACUTE PANCREATITIS IN DOGS**

## 1. INTRODUCTION

AP is typified histologically by acinar cell necrosis, interstitial edema, and a neutrophilic infiltrate of the pancreas.<sup>50</sup> These changes are reversible in AP, unless the initial triggers of inflammation persist, and chronic or recurrent inflammation takes place. Interstitial edematous pancreatitis is the mild form, while necrotizing pancreatitis is the more severe form of pancreatitis.<sup>50</sup>

Cerulein, a cholecystokinin (CCK) analogue, when administered at supraphysiologic doses, leads to excessive digestive enzyme secretion resulting in acute edematous pancreatitis.<sup>51-53</sup> Cerulein, acting through the CCK receptors results in exaggerated stimulation of acinar cells, which leads to activation of trypsinogen to trypsin, in the lysosomal protease cathepsin B-dependent manner.<sup>54</sup> Trypsin causes further activation of other pancreatic zymogens to active enzymes. These activated enzymes within the acinar cells cause autodigestion and subsequently, inflammation of the pancreas. Cerulein-induced AP has been studied extensively in animal models due to its rapid induction, lack of invasiveness, high repeatability, high applicability, and AP-like histologic changes.<sup>36,51-53,55,56</sup> This model also allows investigation of healing and regeneration of damaged tissues after insult termination.<sup>57</sup> US and endoscopic US findings in experimentally induced pancreatitis in dogs have been described.<sup>52,53</sup>

Thus, the purpose of chapter 2 was (1) to determine the feasibility of using quantitative CEUS to detect pancreatic perfusional changes, with the duodenum as an internal control, in cerulein-induced AP in dogs and (2) to describe the patterns of change over time. Pancreatic perfusion after induction of AP was compared to saline controls (before and after saline infusion) as well as before cerulein infusion. It was hypothesized that quantitative CEUS could detect changes in pancreatic perfusion after induction of AP and, if this

hypothesis were to be true, quantitative CEUS would have the potential to be an additional tool in diagnosing and monitoring disease progression in canine AP.

## **2. MATERIALS AND METHODS**

### **2.1 Animals**

Six adult female Beagles, 1 to 2 years old, and weighing 9.5 to 11.3 kg were used in this study. The dogs were healthy based on physical examination findings and normal complete blood count (CBC) and serum biochemistry (including lipase and C-reactive protein). B-mode US identified no evidence of focal or diffuse abnormalities of the pancreas and duodenum in the dogs. All procedures were approved by the Hokkaido University Animal Care and Use Committee.

### **2.2 Cerulein-induced acute pancreatitis**

AP was induced with continuous IV infusion of 7.5  $\mu\text{g}/\text{kg}/\text{h}$  of cerulein (Caerulein; Bachem AG, Bubendorf, Switzerland) in saline into the cephalic vein at a rate of 3 mL/kg/h for 2 hours.<sup>51-53,56</sup> The dogs were observed for the presence of clinical signs associated with AP, such as vomiting and diarrhea. Food was withheld for 24 hours after the start of cerulein infusion and then was slowly reintroduced. As control, all animals received a 2-hour IV infusion of saline at 3 mL/kg/h 2 weeks before cerulein treatment.

### **2.3 B-mode US and CEUS**

#### **2.3.1 Scanning and anesthetic protocols**

US and CEUS examinations were performed before (0 hour) and at 2, 4, 6, and 12 hours after the start of saline and cerulein treatments. Scanning was performed under anesthesia with propofol (Propofol Mylan; Mylan Inc., Canonsburg, Pa, U.S.A.) at an induction dosage of 6 mg/kg and a maintenance rate of 0.4 - 0.6 mg/kg/min,<sup>58</sup> administered to effect using a syringe pump (Top-5300; Top, Tokyo, Japan). For US examinations, dogs were

positioned in left lateral recumbency, and the right pancreatic lobe and descending duodenum adjacent to the right pancreas were identified using an intercostal approach. CEUS examinations of the right pancreatic lobe and descending duodenum adjacent to right pancreas was then performed as described in chapter 1. The duodenum was imaged with the pancreas to determine its suitability as an internal control. Scanning was done continuously for 7 minutes from the start of continuous infusion of MB contrast agent, for generation of a TIC.

During each CEUS examination, MB contrast agent (Sonazoid®; Daiichi-Sankyo, Tokyo, Japan) at a dosage of 0.05 mL/kg diluted in 5 mL of saline was administered as a continuous infusion over one minute as described in chapter 1. The infusion was administered through a 21 G butterfly catheter attached to a 22 G IV catheter placed in a separate cephalic vein from that used for propofol infusion.

### **2.3.2 Settings**

B-mode US and CEUS settings are as detailed in chapter 1.

### **2.4 Quantitative analysis**

Quantitative analysis of CEUS images was performed as described in chapter 1. One image per second for the first 120 seconds followed by 1 image at an interval of every 10 seconds until 420 seconds from the start of MB contrast agent infusion was analyzed. Tissue intensity was measured for each ROI containing 300-600 pixels,<sup>19,59</sup> placed in the pancreatic parenchyma and duodenal mucosa (Fig. 6A). TICs (Fig. 7), depicting the change in tissue intensity over time in the ROI, were created for each CEUS imaging performed before (0 hour), and 2, 4, 6, and 12 hours after saline or cerulein infusion. From these TICs, blood flow velocity as a function of time parameters and blood volume as a function of intensity parameters were evaluated. Measured time parameters included TTU and T<sub>p</sub>, reflecting

wash-in and TTW, reflecting wash-out of MBs from the ROI. PI and area under the curve (AUC) are intensity parameters, the first quantitatively measuring maximum contrast enhancement within the ROI and the second corresponding to the amount of MB flowing through the tissue over a certain time period within the observed ROI.

## **2.5 Statistical analysis**

A statistical analysis program (JMP Pro 10; SAS Institute Inc., Cary, NC) was used to develop a linear mixed model, with time (0, 2, 4, 6, and 12 hours), treatment (saline versus cerulein), and their interaction as categorical fixed effects, and dog identity as random effect. The *F* test was performed to assess the effect of time and treatment on the values of the measured parameters. Pairwise comparisons between times and between treatments were performed by obtaining least squares (LS) means and using Bonferroni correction to account for multiple comparisons. For all analyses, *P*-values of  $< 0.05$  were considered statistically significant.

## **3. RESULTS**

### **3.1 Cerulein-induced acute pancreatitis**

AP was induced in all 6 dogs, as shown by presence of clinical signs and increased serum lipase activity after cerulein infusion (data not shown). Within 20 minutes of beginning cerulein infusion, all dogs exhibited clinical signs associated with AP, such as vomiting (6/6), abdominal discomfort (4/6) and diarrhea (2/6). These clinical signs were mostly observed during the 2 hours of cerulein infusion. Vomiting ceased after the end of cerulein infusion. All dogs recovered from AP without complications within 1 to 2 days, as shown by complete resolution of clinical signs and normalization of serum lipase activity.

### **3.2 US findings**

In all dogs, pancreatic lesions were most apparent 2 to 4 hours after start of cerulein infusion, and included glandular swelling, well-defined interlobular anechoic fissures, and subcapsular anechoic spaces. All dogs showed severe swelling at 2 hours, whereas 3/6 showed severe and 3/6 showed moderate swelling at 4 hours. In all but 1 dog, mild corrugation of the duodenum was seen at different time points after start of cerulein infusion. With time, the lesions became less severe, and by 12 hours the pancreatic lesions described above were no longer apparent apart from some swelling (2/6 mild, 1/6 moderate). Hyperechoic mesentery was observed in 3/6 dogs at 2 hours and in all dogs at 4 hours. No peripancreatic fluid accumulation was observed at any time point. There were no observable changes in the pancreas or duodenum in saline controls.

### **3.3 CEUS findings**

At 0 hour (before saline or cerulein infusion), the CrPDA was enhanced earliest, followed by the pancreatic parenchyma, and then duodenal mucosa. The increase in tissue enhancement was gradual until it reached PI (Fig. 6A), followed by a plateau. Thereafter, there was progressive wash-out of the contrast agent with gradual loss of tissue enhancement. Subjectively, the parenchyma of the pancreas and duodenum could not be seen clearly when the intensity decreased to approximately 30 MPV.

In cerulein treatment, CEUS changes in the pancreas were most apparent 2 to 4 hours after infusion and became less severe with time. Subjectively, the pancreatic parenchyma showed similar gradual increase in echogenicity, but was more intensely enhanced at PI when compared to 0 hour (before cerulein infusion, Fig. 6B). The CrPDA and CrPDV were more prominent, and fine pancreatic capillaries were visible. The swollen pancreatic parenchyma was separated by anechoic interlobular fissures that were unenhanced. Similarly, subcapsular edema also was unenhanced. The pancreatic parenchyma was hyperechoic for a longer duration with delayed wash-out when compared to 0 hour (before cerulein infusion). There were no observable changes in the wash-in speed or  $T_p$ . The order of tissue enhancement remained unchanged from 0 hour (before saline or cerulein infusion) with the pancreas enhancing before the duodenum in all dogs. With saline treatment,  $T_p$  was slightly faster 2 hours after the start of saline infusion. There were no other observable changes in pancreatic enhancement. Changes to the intensity or time parameters of the duodenal mucosa after saline or cerulein treatments were not observed.

### **3.4 Statistical analysis**

Measured parameters of the pancreas and duodenum are summarized in Table 2. For the pancreas, significant interaction between treatment and time was found for PI ( $P < 0.05$ ). Dogs subjected to cerulein treatment had significantly higher PI at 2 (least squares [LS]

means, 101 MPV; 95% confidence interval (CI), 89 to 113 MPV;  $P < 0.01$ ) and 4 hours (LS means, 99 MPV; 95% CI, 88 to 111 MPV;  $P < 0.01$ ) compared to baseline PI at 0 hour (LS means, 83 MPV; 95% CI, 71 to 94 MPV). Pairwise comparisons of specific treatment-time combinations identified a significant treatment effect at 2 (saline treatment LS means, 78 MPV; 95% CI, 67 to 90 MPV;  $P < 0.001$ ), 4 (saline treatment LS means, 79 MPV; 95% CI, 67-90 MPV;  $P < 0.001$ ), and 6 hours (cerulein treatment LS means, 92 MPV; 95% CI, 80-104 MPV vs saline treatment LS means, 77 MPV; 95% CI, 66 to 89 MPV;  $P < 0.05$ ).

AUC for cerulein treatment followed a time course similar to PI. Significant interaction between treatment and time was detected for AUC ( $P < 0.05$ ). A significant time effect relative to 0 hour was identified at 4 hours (LS means, 19,700 MPV\*s; 95% CI, 16,200 to 23,100 MPV\*s;  $P < 0.01$ ) for cerulein treatment. Pairwise comparisons of specific treatment-time combinations identified a significant treatment effect at 4 (saline treatment LS means, 12,000 MPV\*s; 95% CI, 8,600 to 15,500 MPV\*s;  $P < 0.001$ ) and 6 hours (cerulein treatment LS means, 18,000 MPV\*s; 95% CI, 14,600 to 21,500 MPV\*s vs saline treatment LS means, 12,600 MPV\*s; 95% CI, 9,100 to 16,000 MPV\*s;  $P < 0.01$ ).

TTW showed significant treatment and time interaction ( $P < 0.05$ ). A significant difference between the cerulein (LS means, 295 s; 95% CI, 257 to 333 s;  $P < 0.05$ ) and saline treatment (LS means, 210 s; 95% CI, 172 to 248 s) at 4 hours was observed. For saline treatment, significant time effect was found for Tp at 2 hours (LS means, 48 s; 95% CI, 42 to 54 s;  $P < 0.05$ ) when compared to 0 hour (LS means, 61 s; 95% CI, 55 to 66 s). No significant differences were observed for TTU. Measured parameters for the duodenum did not exhibit any significant differences for both saline and cerulein treatments.

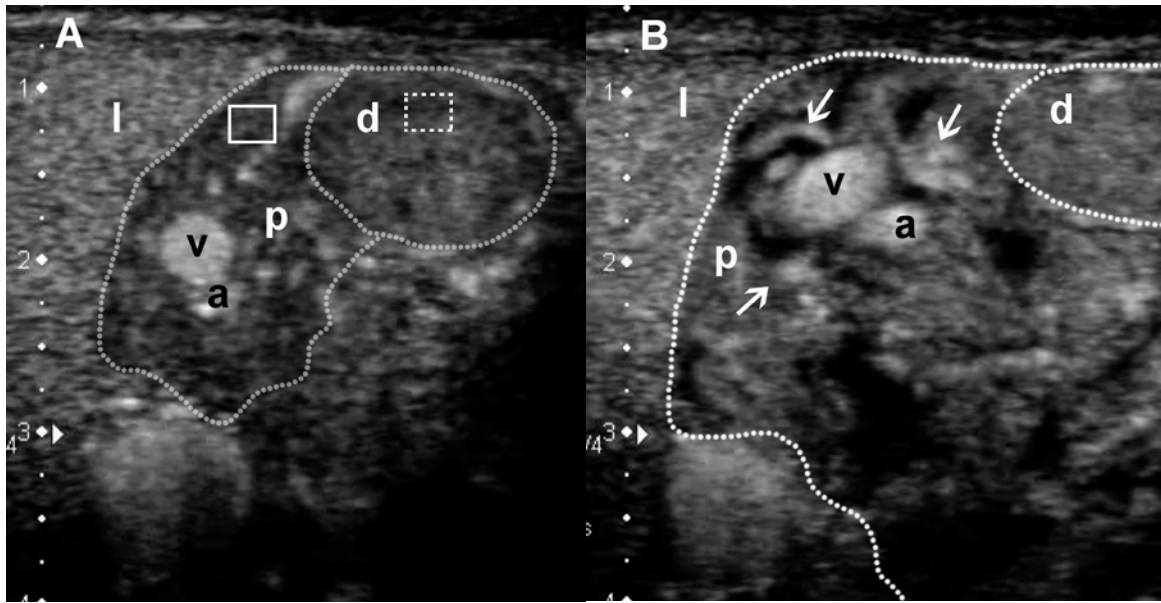


Figure 6. CEUS images of the transverse view of the right pancreatic lobe (p), and mucosa of the descending duodenum adjacent to the right pancreas (d) (both outlined by dotted lines) at peak enhancement in a representative dog (dorsal to the left, ventral to the right, medial to the bottom, and scales in cm to the left). (A) Before cerulein treatment (0 hour). Image acquired 59 seconds after the start of contrast agent infusion showing non-homogeneous enhancement of pancreatic parenchyma and duodenal mucosa. The pancreas is demarcated from the adjacent liver (l). The CrPDA (a) and CrPDV (v) also are enhanced at this time. ROIs are placed manually in the pancreatic parenchyma (solid box) and duodenal mucosa (dashed box) to measure tissue intensity. (B) 2 hours after start of cerulein treatment. Image acquired 58 seconds after contrast agent infusion. The pancreatic parenchyma is more intensely enhanced when compared to 0 hour. The CrPDA and CrPDV are more prominently enhanced and fine capillaries (arrows) are visible. The swollen pancreatic parenchyma is separated by interlobular fissures and subcapsular edema that were unenhanced.

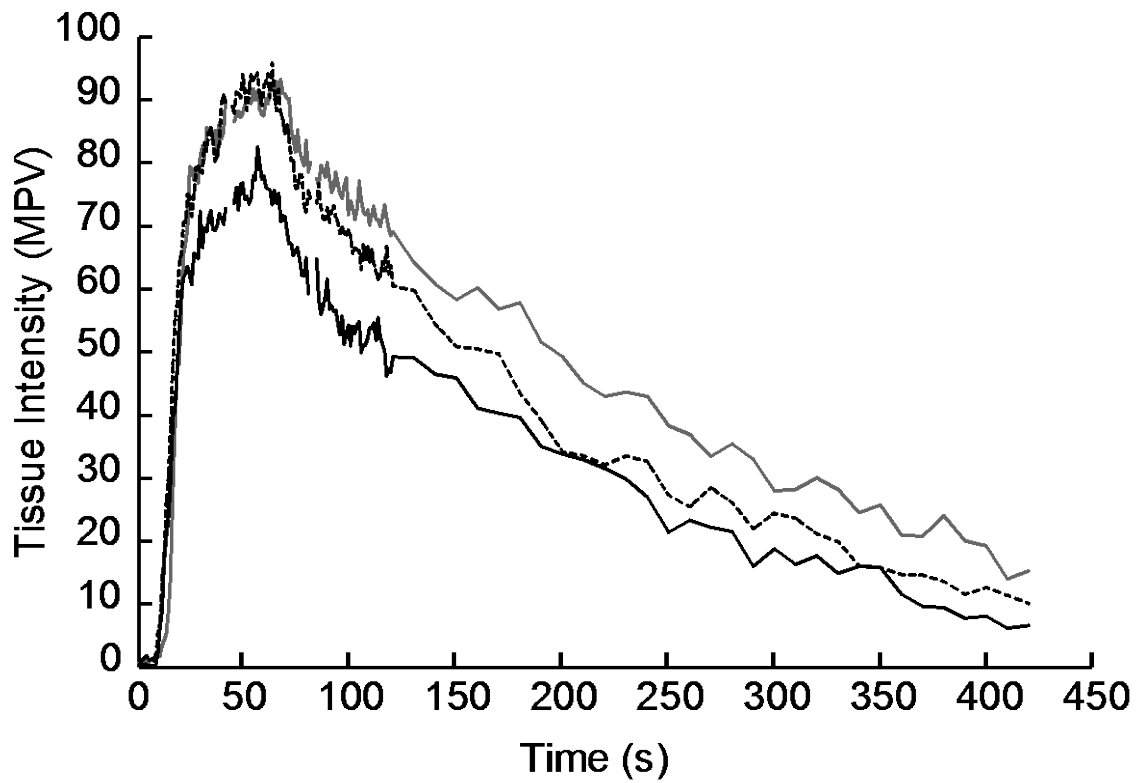


Figure 7. TICs showing the mean pixel intensity of the pancreatic parenchyma before (0 hour, solid black line), 2 (dashed black line), and 4 hours (dashed gray line) after cerulein infusion (n = 6). The curves are of the similar shape, but are higher at 2 and 4 hours when compared to 0 hour. The wash-out at 4 hours is more gradual when compared to 0 and 2 hours. MPV, Mean pixel value.

**Table 2.** Least squares means (95% confidence intervals) obtained from the linear mixed model for measured parameters from TICs before (0 hour), 2, 4, 6, and 12 hours after saline and cerulein treatment (n = 6)

Measured Parameters, by Location	Time (hour)									
	Saline treatment					Cerulein treatment				
Pancreas	0	2	4	6	12	0	2	4	6	12
PI (MPV)	78 (66- 90)	78 (67- 90)	79 (67- 90)	77 (66- 89)	78 (66- 90)	83 (71- 94)	101 (89- 113) <sup>a, c</sup>	99 (88- 111) <sup>a, c</sup>	92 (80- 104) <sup>b</sup>	86 (74- 98)
AUC (MPV*s)	12,200 (8,800- 15,700)	13,100 (9,700- 16,500)	12,000 (8,600- 15,500)	12,600 (9,100- 16,000)	12,700 (9,300- 16,200)	14,000 (10,600- 17,500)	17,000 (13,600- 20,500)	19,700 (16,200- 23,100) <sup>a, c</sup>	18,000 (14,600- 21,500) <sup>a</sup>	15,300 (11,900- 18,800)
TTU (s)	18 (16- 20)	16 (14- 18)	18 (16- 20)	20 (17- 22)	19 (17- 21)	15 (13- 17)	14 (12- 17)	18 (16- 20)	17 (14- 19)	17 (15- 19)
Tp (s)	61 (55- 66)	48 (42- 54) <sup>d</sup>	64 (58- 69)	60 (55- 66)	56 (50- 62)	58 (52- 64)	56 (50- 61)	60 (54- 65)	60 (55- 66)	58 (53- 64)
TTW (s)	232 (192- 271)	232 (192- 271)	210 (171- 249)	238 (199- 278)	217 (177- 256)	232 (192- 271)	230 (191- 269)	295 (256- 334) <sup>a</sup>	288 (250- 326)	243 (204- 283)

Duodenum	0	2	4	6	12	0	2	4	6	12
PI (MPV)	70 (55- 79)	75 (63- 87)	70 (57- 82)	71 (59- 83)	74 (62- 86)	77 (65- 89)	81 (69- 93)	78 (66- 90)	85 (73- 97)	75 (63- 87)
AUC (MPV*s)	9,000 (6,000- 12,000)	9,900 (7,000- 12,900)	9,000 (6,000- 12,000)	10,100 (7,200- 13,100)	10,000 (7,000- 12,900)	11,700 (8,700- 14,600)	11,000 (8,000- 14,000)	12,300 (9,400- 15,300)	13,300 (10,300- 16,200)	11,500 (8,500- 14,400)
TTU (s)	21 (17- 23)	19 (16- 21)	20 (19- 23)	23 (20- 25)	22 (19- 24)	17 (15- 20)	18 (15- 20)	19 (16- 21)	18 (16- 21)	21 (19- 24)
Tp (s)	63 (58- 68)	58 (53- 63)	62 (57- 66)	65 (60- 70)	61 (56- 66)	62 (58- 67)	51 (47- 56)	57 (52- 62)	60 (55- 65)	59 (54- 64)
TTW (s)	193 (144- 241)	197 (149- 245)	182 (134- 230)	200 (152- 248)	218 (170- 266)	208 (160- 256)	171 (123- 219)	218 (170- 266)	218 (170- 266)	225 (177- 273)

PI, Peak intensity; AUC, Area under the curve; TTU, Time to initial upslope; Tp, Peak time; TTW, Time to wash-out; MPV, Mean pixel value.

<sup>a</sup>Significant ( $P < 0.01$ ) treatment effect.

<sup>b</sup>Significant ( $P < 0.05$ ) treatment effect.

<sup>c</sup>Significant ( $P < 0.01$ ) time effect when compared to 0 hour.

<sup>d</sup>Significant ( $P < 0.05$ ) time effect when compared to 0 hour.

## 4. DISCUSSION

AP was successfully induced in the present study. Quantitative CEUS detected perfusion changes in the pancreas of dogs with cerulein-induced AP. Significant changes were observed in the pancreas for the intensity parameters (PI, AUC), reflecting increased blood volume,<sup>18,31</sup> within 2 to 4 hours post-infusion. As a function of blood flow velocity,<sup>18,31</sup> the time parameter TTW was prolonged at 4 hours post-cerulein infusion when compared to saline control at 4 hours, and Tp was faster after 2 hours of saline infusion when compared to baseline values (pre-saline treatment). The intensity parameters of the pancreas normalized to baseline values (pre-cerulein treatment) within 10 hours after termination of cerulein infusion. Although the duodenum showed mild corrugation on B-mode US, no changes in intensity or time parameters were detected on CEUS.

Infusion of supraphysiological doses of cerulein results in the development of acute edematous pancreatitis in many animal models including the dog.<sup>36,51-53,56</sup> This noninvasive method produces consistent histologic and B-mode US findings within 2 to 4 hours of infusion.<sup>36,52,53,56</sup> In the current study, these B-mode US findings were reproducible, and were consistent with previous reports with changes seen most dramatically in the pancreas from 2 to 4 hours after cerulein treatment.

CEUS uses MB, which are blood-pool contrast agents. Although the capillary network is not anatomically visible in CEUS, MB in the microvasculature can be perceived as contrast-enhancement with echogenicity dependent on the amount of MB in the ROI.<sup>60</sup> CEUS provides real-time information corresponding with the perfusion dynamics of the pancreas and disease progression in the AP patient.<sup>32</sup> B-mode US provides useful information on the appearance of the pancreas, but it is highly subjective and dependent on the

assessment and experience of each ultrasonographer. Quantification of echogenicity on CEUS using TIC provides additional objective assessment of the perfusional changes in the pancreas.

In this study, the increased intensity parameters can be attributed to microvascular changes seen in the inflamed pancreas. Previous studies showed that pancreatic microvascular changes in cerulein-induced AP are seen within 2 hours of cerulein infusion, and include gross reduction in the number of capillaries and dilatation of the remaining microvasculature.<sup>56,61</sup> In one study using scanning and transmission electron microscopy to demonstrate microvascular derangements, capillaries with obliterated ends and irregular arrangements were observed.<sup>56</sup> Previous CEUS studies in both the human and veterinary medical literature showed increased echogenicity in the inflamed pancreatic parenchyma.<sup>29,35</sup> Increased pancreatic PI in cerulein-induced AP could be due to accumulation of trapped MBs in the obliterated ends of the capillaries in addition to MB flowing into the pancreas. Slower wash-out of these trapped MB resulted in prolonged TTW and higher AUC values corresponding with visually prolonged hyperechoic enhancement of the inflamed pancreas. In the present study, the increase in intensity parameters therefore reflects the increased blood volume in the inflamed pancreas that not only is due to hyperemia,<sup>62</sup> but to some extent congestion as evidenced by prolonged wash-out of the contrast agent. In contrast, saline infusion did not increase pancreatic blood flow as demonstrated by unchanged values of the intensity parameters, PI and AUC.

In the present study, faster Tp at 2 hours post-saline infusion could be due to increased pancreatic circulation from fluid therapy.<sup>63</sup> In the pancreas of cerulein-induced AP, Tp at 2 hours was slower than saline control, but did not differ from 0 hour (pre-cerulein treatment). One would expect Tp to be delayed when compared to 0 hour (pre-cerulein treatment) due to slower velocity of blood flow in dilated and tortuous blood vessels,<sup>64</sup>

because more time is needed for MB to accumulate to PI. However, these effects could have been countered by the simultaneous infusion of saline with cerulein.

In contrast to a previous report with no secondary duodenal lesions seen on B-mode US,<sup>52</sup> corrugation of the duodenum was seen at different times post-cerulein infusion in this study. However, no changes in CEUS were seen in the duodenum for both intensity and time parameters with cerulein or saline treatment although a similar pattern of decreased Tp was seen at 2 hours post-saline infusion. This could be explained by the absence of microcirculatory derangements in the duodenum from the local inflammatory effects of pancreatitis, probably due to the short duration of cerulein infusion in the current study. Presence of duodenal corrugation also is a non-specific US finding that could be present due to various diseases such as pancreatitis, enteritis, or peritonitis.<sup>49</sup> Furthermore, improvements in US technology and presence of observer bias due to lack of blinding to treatments (saline or cerulein infusion) may have contributed to detection of duodenal corrugations in this study.

A few limitations were present in the current study. Firstly, cerulein-induced AP only results in a mild form of pancreatitis that does not lead to necrosis.<sup>36,52,57</sup> This may explain the difference between CEUS findings in the present study and those previously reported in naturally occurring pancreatitis in dogs. The current study identified a hyperperfused pancreas, whereas the previous study disclosed hypoperfused or non-enhanced lesions within the pancreas.<sup>34</sup> The ultrasonographic appearance of interlobular edema in this pancreatitis model also is not seen commonly in naturally occurring pancreatitis in dogs.<sup>52</sup> This suggests that this model may not completely reflect the pathogenesis of clinical pancreatitis, or that animals rarely are presented this soon after the onset of inflammation. Additional research in the application of CEUS in detecting naturally occurring pancreatitis and in differentiating focal lesions in pancreatic cancer and mass-forming pancreatitis is warranted. Secondly, because of the short time intervals between subsequent CEUS examinations, pancreatic

biopsy could not be performed in the current study without causing more inflammation therefore confounding the effects of cerulein treatment alone.

CEUS applications in abdominal tumors and pancreatic masses evaluate the perfusional differences of the suspicious region from surrounding macroscopically normal regions.<sup>14,16,28,30,31</sup> However, in pancreatitis, a visually normal pancreatic area for internal control is difficult to identify. Thus, in this study, the descending duodenum was imaged with the pancreas to determine its suitability as an internal control. No CEUS changes were observed in the duodenum in this study. As reported in chapter 1, PI of the canine pancreas is only slightly higher than that of the duodenum on CEUS with continuous infusion of contrast MB.<sup>59</sup> Thus, real-time visual comparison of the pancreatic parenchyma with the duodenal mucosa for increased hyperechogenicity during the CEUS examination could be done.

In conclusion, CEUS can be used in the dog for detecting microvascular derangements as a possible sign of pancreatic inflammation. Quantifying the intensity parameters, namely PI and AUC, as a function of blood volume can provide valuable information in differentiating acute edematous pancreatitis from normal pancreatic tissue. Cerulein-induced AP was characterized by prolonged hyperechoic enhancement on CEUS.

## 5. SUMMARY

In this chapter, the feasibility of using quantitative CEUS to detect pancreatic perfusional changes in cerulein-induced AP in dogs was investigated. In cerulein-induced AP, pancreatic PI increased at 2 and 4 hours when compared to 0 hour, and at 2, 4, and, 6 hours when compared to control. AUC increased at 4 hours when compared to 0 hour, and at 2 and 4 hours when compared to control. TTW was prolonged at 4 hours when compared to control. For saline control, peak time was faster at 2 hours when compared to 0 hour. CEUS parameters PI and AUC can provide useful information in differentiating AP from normal pancreas. Cerulein-induced AP was characterized by prolonged hyperechoic enhancement on CEUS.

## **CHAPTER 3**

# **QUANTITATIVE CONTRAST-ENHANCED ULTRASONOGRAPHIC ASSESSMENT OF NATURALLY OCCURRING PANCREATITIS IN DOGS**

## 1. INTRODUCTION

Advanced diagnostic imaging modalities such as CT and magnetic resonance imaging have been used to evaluate and characterize severity of pancreatitis in people.<sup>65</sup> The use of CT in the diagnosis of pancreatitis in dogs has been reported in a small number of dogs.<sup>34,66</sup> Recently, a new development in CT imaging called perfusion CT has shown usefulness in detecting changes in pancreatic perfusion in various pathologies (including inflammation and neoplasia) in people.<sup>67-69</sup> The usefulness of this technique has not yet been evaluated in veterinary medicine. However, general anesthesia or deep sedation is needed for CT examination in veterinary patients. CEUS, a less invasive diagnostic test, has been reported to be comparable to CT in the assessment of AP in people.<sup>32</sup>

In the previous chapter, I have demonstrated the feasibility of using quantitative CEUS to detect pancreatic perfusion changes in experimentally induced AP in dogs. Experimentally induced AP is characterized by prolonged hyperechoic enhancement on CEUS.<sup>70</sup>

In chapter 3, I aimed to determine the feasibility of using quantitative CEUS to detect pancreatic and secondary duodenal perfusion changes in naturally occurring canine pancreatitis. It was hypothesized that quantitative CEUS could detect pancreatic and secondary duodenal perfusion changes, as a possible sign for presence of inflammation in naturally occurring pancreatitis in dogs. If this hypothesis were to be true, quantitative CEUS would potentially be useful as a new diagnostic tool in diagnosing pancreatitis in dogs.

## **2. MATERIALS AND METHODS**

### **2.1. Patients**

This study was performed with approval from the Hokkaido University Animal Care and Use Committee. Twenty-three client-owned dogs that were presented to Hokkaido University Veterinary Teaching Hospital between September 2011 and December 2013 for pancreatitis were prospectively enrolled. Diagnosis of pancreatitis was based on 1) presence of 1 or more acute clinical signs (< 2 weeks) (e.g., vomiting, anorexia, lethargy) and 1 or more physical examination findings associated with pancreatitis (e.g., abdominal pain, jaundice, dehydration), 2) abnormal pancreatic lipase immunoreactivity (Spec cPL > 400 µg/L), and 3) presence of 1 or more abdominal US findings consistent with pancreatitis (e.g., enlarged, irregular, hypoechoic pancreas with surrounding hyperechoic mesentery). Inclusion criteria were: owner's consent and unobstructed visualization of pancreas on US. Exclusion criterion was presence of other primary diseases (e.g. gastrointestinal, hepatobiliary, urinary) that may be responsible for the clinical signs.

To obtain reference parameters, data from 12 normal controls (including 8 normal controls from chapter 1) were included. These laboratory-owned dogs (7 mixed-breed and 5 Beagle) were healthy based on physical examination findings, normal CBC and serum biochemistry (including lipase and C-reactive protein), and abdominal US findings.

### **2.2 B-mode US and CEUS**

#### **2.2.1 Location**

The clinician responsible for the case performed the B-mode US examination. A different operator (LSY), who was not blinded to the US findings, performed the CEUS

examination. CEUS was performed following at least a 6-hour fast. The location for CEUS imaging was predetermined during the initial B-mode US. If the pancreatic abnormality was generalized or localized to the right lobe, CEUS of the right pancreatic lobe was performed using a right intercostal approach. The adjacent descending duodenum was imaged simultaneously with the right pancreatic lobe, in a single US view, to investigate secondary perfusion changes in the duodenum. If pancreatic abnormality was localized elsewhere (pancreatic body or left lobe), CEUS of that area was performed instead.

### **2.2.2 Settings**

B-mode US and CEUS settings are as detailed in chapter 1.

### **2.2.3 Contrast agent**

MB contrast agent (Sonazoid®; Daiichi-Sankyo, Tokyo, Japan) at a dosage of 0.05 mL/kg diluted in 3 mL (dogs < 3 kg) or 5 mL (dogs > 3 kg) of saline was administered as a continuous infusion over one minute as described in chapter 1. Scanning was performed for 5 minutes from the start of contrast agent infusion for generation of a TIC.

## **2.3 Quantitative analysis**

A single operator (LSY) performed the quantitative analysis of the CEUS images as described in chapter 1. One image per second for the first 2 minutes followed by 1 image at an interval of every 10 seconds until 300 seconds from the start of MB contrast agent infusion was analyzed. In each image, a ROI containing 300-600 pixels,<sup>19</sup> was manually placed in the pancreatic parenchyma and duodenal mucosa (if available) for measurement of tissue intensity. TICs (Fig. 8) were created and perfusion parameters (time and intensity) as described in chapter 2 were measured. AUC was measured over 300 seconds.

## **2.4 Statistical analysis**

Statistical analysis programs (JMP Pro 10; SAS Institute Inc., Cary, NC and SAS 9.2; SAS Institute Inc., Cary, NC) were used for statistical analysis. Normality of data was assessed using kurtosis and skewness. When distribution approached normality, measured parameters of the pancreas and duodenum from dogs with pancreatitis and controls were compared using Student's *t*-test and Bonferroni correction was applied to account for multiple comparisons. Non-normally distributed data were compared using Wilcoxon rank sum test. Receiver operating characteristic (ROC) curves were constructed to determine the optimal cutoff values for each measured parameter of the pancreas. To compare the performance of these parameters, the area under the ROC curves (AUROC) were compared using the method of DeLong.<sup>71</sup> The most optimal cut-off value was determined by the one with highest Youden's Index. The cutoff values obtained were applied and sensitivities and specificities were calculated for each measured parameter. A *P*-value of < 0.05 was considered statistically significant.

## 3. RESULTS

### **3.1 Animals**

A total of 23 dogs satisfying the inclusion criteria were recruited. Signalment of dogs in the pancreatitis and control group is summarized in Table 3. Dogs in the pancreatitis group were significantly older and weighed less than dogs in the control group ( $P < 0.001$  and  $P = 0.0012$ , respectively). The most common clinical sign was anorexia or inappetence (21/23; 91%), followed by lethargy (19/23; 83%), vomiting (15/23; 65%), weight loss (11/19; 58%), and diarrhea (13/23; 57%). Selected serum biochemistry results of dogs in the pancreatitis and control group are summarized in Table 3. Ninety-one percent (21/23) of dogs had concurrently increased lipase activity, C-reactive protein, and Spec cPL value  $> 400 \mu\text{g/L}$ .

### **3.2 B-mode US**

Ultrasonographic abnormalities were observed in the right pancreatic lobe in 22 dogs, body in 10 dogs, and left lobe in 6 dogs. The pancreatic parenchyma was diffusely hypoechoic in 9 dogs, diffusely hyperechoic in 2 dogs, and inhomogeneous in 12 dogs. In one dog, a hypoechoic area with irregular margin was observed within the pancreatic parenchyma. 22 dogs had enlarged pancreas, 20 had irregular pancreatic margins, 10 had hyperechoic peripancreatic mesentery, and 10 had duodenal corrugations.

### **3.3 CEUS findings**

CEUS was performed at the right pancreatic lobe and adjacent descending duodenum in 21/23 dogs, right pancreatic lobe only and pancreatic body in each of the remaining two dogs. CEUS was performed without sedation in control dogs. In the pancreatitis group, six dogs received analgesia as part of treatment for pancreatitis before CEUS. CEUS images of

the pancreas in 20 dogs with pancreatitis and 12 control dogs were satisfactory, and were included for quantitative analysis. CEUS images of the duodenum in 18 dogs with pancreatitis and 9 control dogs were satisfactory, and were also included for quantitative analysis. CEUS data from three dogs with pancreatitis were excluded from quantitative analysis due to CEUS of insufficient quality (n = 2) and inability to visualize the pancreas during the entire duration of CEUS (n = 1).

The TIC (Fig. 8) of the pancreas in the pancreatitis group differed from the control group, and corresponded with perfusion changes observed visually. In the control group, the craniopancreaticoduodenal artery was enhanced first, followed by the pancreatic parenchyma, and then duodenal mucosa. Contrast wash-in to PI was gradual, followed by a plateau, and then a slow wash-out was observed. In the pancreatitis group, this order of enhancement was unchanged. However, contrast wash-in to PI was delayed. The pancreatic parenchyma was intensely enhanced for a longer period of time, resulting in a slower wash-out. In some dogs, fine pancreatic capillaries within the pancreatic parenchyma were more prominently enhanced when compared to control dogs. (Fig. 9A). The duodenum, which was simultaneously imaged with the pancreas, was also more intensely enhanced with a prolonged wash-out in dogs with pancreatitis compared to control dogs. Visually, PI of the duodenum was not different from the pancreas.

In four dogs, non-enhancing lesions suggestive of areas of necrosis were observed (Fig. 9B). A single non-enhancing lesion was seen in two dogs, while multiple non-enhancing lesions were observed in the remaining two dogs. However, histopathology confirmation was not available in this study. Dimensions of these non-enhancing lesions on CEUS were smaller in two dogs, similar in one, and larger in one when compared to the corresponding hypo- to isoechoic pancreatic area on B-mode US.

### **3.4 Statistical analysis**

Values of measured parameters, reflecting pancreatic and duodenal perfusions are summarized in Table 4. For the pancreas, Tp of the pancreatitis group was significantly prolonged when compared to control group ( $P < 0.001$ ). TTW prolonged in the pancreatitis group but was not significant ( $P = 0.47$ ). PI and AUC were also significantly increased when compared to control group ( $P < 0.01$  and  $P < 0.05$ , respectively). For the duodenum, PI and AUC were significantly increased when compared to control group ( $P < 0.01$  and  $P < 0.05$ , respectively).

Table 5 shows the results of the ROC analysis. Tp produced the highest value for the area under ROC curve (AUROC) followed by PI and AUC. Cutoffs were determined based on the ROC curves.  $Tp \geq 48$  s resulted in sensitivity value of 90% and specificity value of 83% in detecting presence of pancreatitis.  $PI \geq 87$  MPV resulted in sensitivity value of 80% and  $AUC \geq 13,700$  MPV\*s resulted in specificity value of 83%.

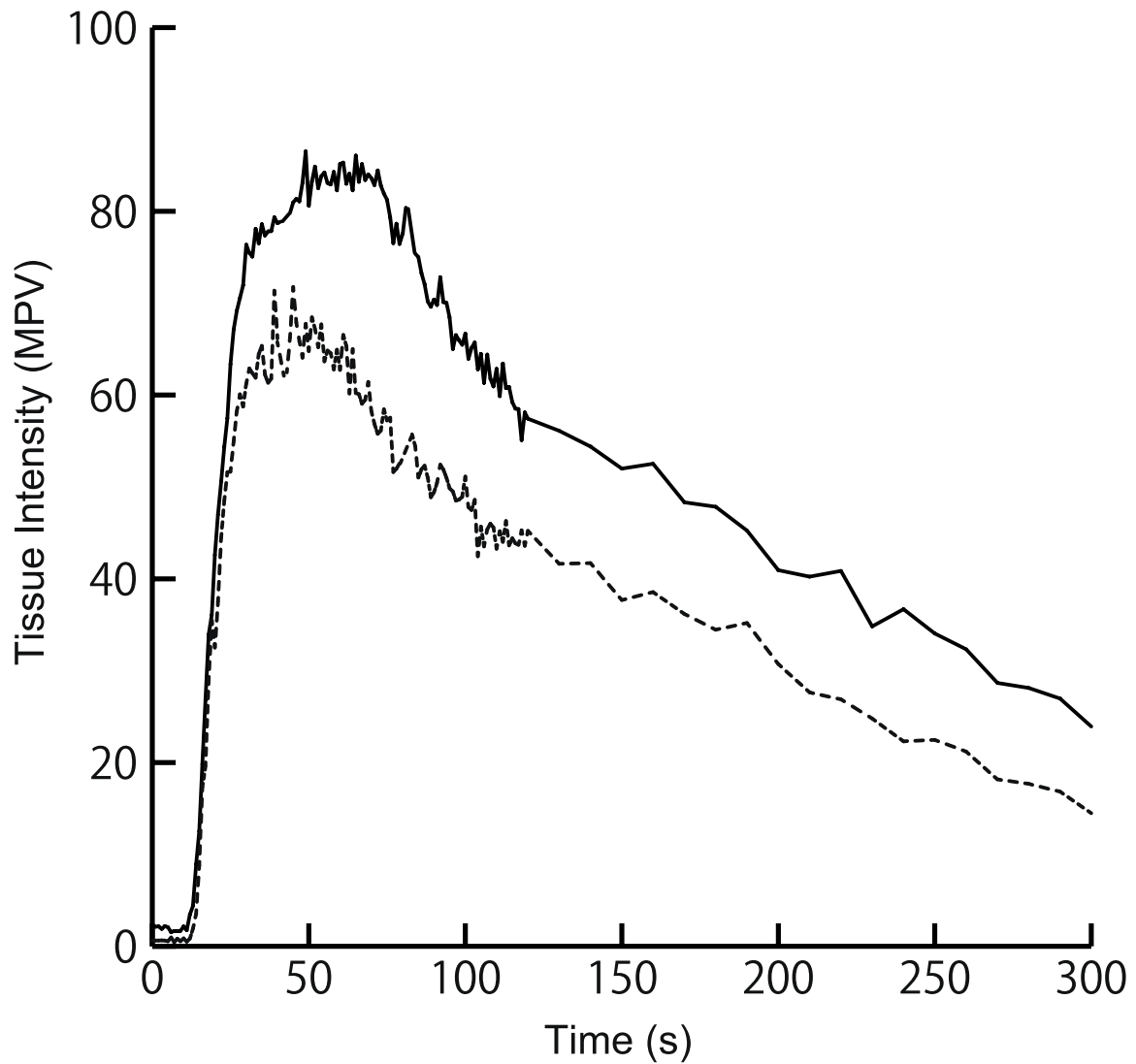


Figure 8. TICs showing the mean pixel intensity in the pancreatic parenchyma of pancreatitis group (solid black line, n = 20) and control group (dashed black line, n = 12). TIC of the pancreatitis group is similar in shape, but is higher in intensity, and peaked at a later time when compared to control group. The wash-out is also more gradual in the pancreatitis group. MPV, Mean pixel value.

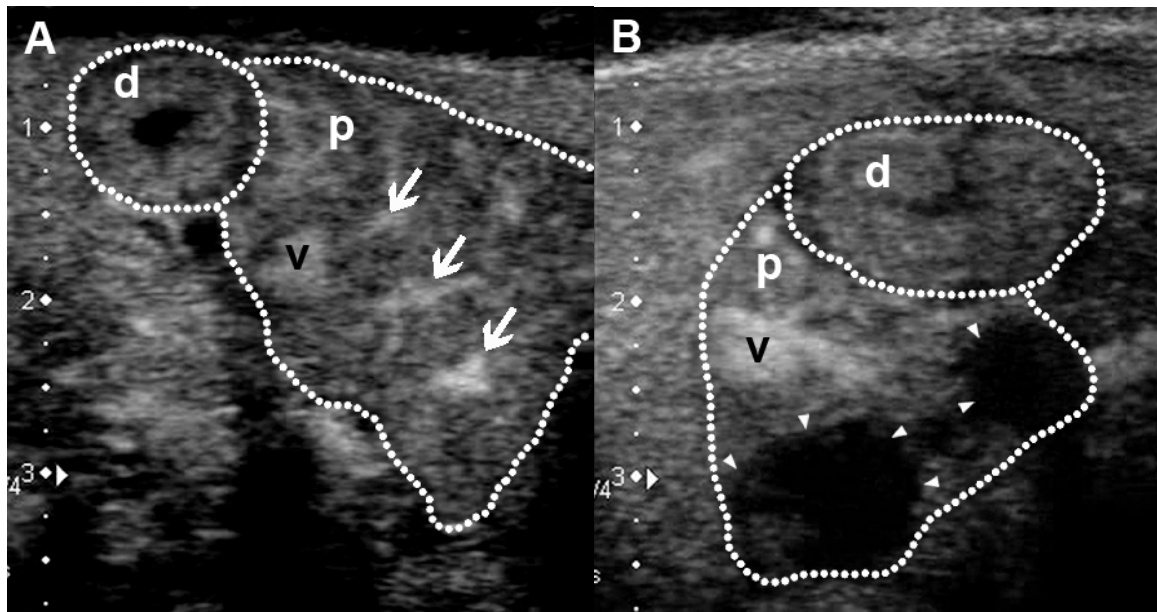


Figure 9. CEUS images of the transverse view of the right pancreatic lobe (p) and mucosa of the descending duodenum adjacent to the right pancreas (d) (both outlined by dotted lines) in 2 representative dogs with pancreatitis (dorsal to the left, ventral to the right, medial to the bottom, and scales in cm to the left). (A) Image acquired at 69 s after start of contrast agent infusion showing the pancreas at PI. The pancreas is swollen with irregular outlines, and is enhanced non-homogeneously. Apart from the CrPDV (v) normally seen, fine pancreatic capillaries are also more prominently enhanced (arrows). Clinical signs of vomiting ceased and activity improved after 4 days of hospitalization and medical therapy. Lipase activity returned to normal range within 10 days. (B) Image acquired at 67 s after start of contrast agent infusion showing 2 non-enhancing lesions (arrowheads) in the pancreatic parenchyma. This dog recovered from the acute episode of pancreatitis and was discharged after 10 days of hospitalization and medical therapy. However, lipase activity and C-reactive protein did not return to normal ranges until 46 and 25 days, respectively.

**Table 3.** Signalment and selected variables from serum biochemistry of dogs in pancreatitis and control group

Signalment	Pancreatitis group (n = 23)	Control group (n = 12)	P-value <sup>e</sup>
Age (years old) <sup>a</sup>	11 (4 – 19)	2 (1 – 7)	< 0.001
Body weight (kg) <sup>a</sup>	4.6 (1.3 – 19.3)	12.8 (9.5 – 18)	0.0012
Sex	5 M, 7 F, 5 CM, 6 SF	6 M, 6 F	NA
Breed	Miniature Dachshund (n = 4), Papillon (3), Maltese (2), Miniature Schnauzer (2), Chihuahua (2), Pembroke Welsh Corgi (2), Pomeranian (2), Mixed-breed (2), American Cocker Spaniel (1), Yorkshire Terrier (1), Basset Hound (1), and Toy Poodle (1)	Mixed-breed (n = 7) and Beagle (5)	NA
Lipase <sup>a,b</sup> (RI: 0 – 160 IU/L)	855 (244 – 1000)	36 (18 – 75)	< 0.001
C-reactive protein <sup>a,c</sup> (RI: 0 – 1 mg/dL)	6.8 (0 – 20)	0.1 (0 – 0.6)	< 0.001
Spec cPL <sup>a,d</sup> (RI: ≤ 200 µg/L)	732 (418 – 1000)	NA	NA

M, Male; F, Female; CM, Castrated male; SF, Spayed female; NA, Not applicable; RI, Reference interval

<sup>a</sup>Values expressed as median (range)

<sup>b</sup>Values above upper detection limit are expressed as 1000 IU/L.

<sup>c</sup>Values above upper detection limit are expressed as 20 mg/dL.

<sup>d</sup>Values above upper detection limit are expressed as 1000 µg/L.

<sup>e</sup>Based on the comparison of pancreatitis and control group using the Wilcoxon rank sum test.

**Table 4.** Mean  $\pm$  standard deviation of pancreatic and duodenal perfusion parameters measured from TIC of dogs from pancreatitis and control group

Measured parameters	Pancreas			Duodenum		
	Pancreatitis group	Control group	P-value <sup>a</sup>	Pancreatitis group	Control group	P-value <sup>a</sup>
	(n =20)	(n = 12)		(n = 18)	(n = 9)	
TTU (s)	19 $\pm$ 4	19 $\pm$ 4	1.00	21 $\pm$ 4	22 $\pm$ 3	1.00
Tp (s)	62 $\pm$ 11	39 $\pm$ 13	< 0.001	61 $\pm$ 9	50 $\pm$ 15	0.13
TTW (s)	268 $\pm$ 69	228 $\pm$ 47	0.47	246 $\pm$ 69	203 $\pm$ 32	0.53
PI (MPV)	95 $\pm$ 15	78 $\pm$ 13	0.009	94 $\pm$ 14	74 $\pm$ 10	0.005
AUC (MPV*s)	14,900 $\pm$ 3,400	11,000 $\pm$ 2,800	0.013	14,000 $\pm$ 4,000	9,700 $\pm$ 2,000	0.045

TTU, Time to initial up-slope; Tp, Peak time; TTW, Time to wash-out; MPV, Mean pixel value; PI, Peak intensity; AUC, Area under the curve

<sup>a</sup>Based on the comparison of pancreatitis and control group using Student's *t*-test and Bonferroni correction to account for multiple comparisons.

**Table 5.** Area under the ROC curves (AUROC) and their 95% confidence intervals (95% CI) for the pancreatic perfusion parameters

Measured parameters	AUROC (95% CI)	Cutoff value	Sensitivity (95% CI) <sup>a</sup>	Specificity (95% CI) <sup>a</sup>
TTU (s)	0.50 (0.29 – 0.71)	≥ 18	65 (43 – 82)	50 (25 – 75)
Tp (s)	0.92 (0.82 – 1.00)	≥ 48	90 (70 – 97)	83 (55 – 95)
TTW (s)	0.64 (0.44 – 0.83)	≥ 250	65 (43 – 82)	67 (39 – 86)
PI (MPV)	0.82 (0.67 – 0.97)	≥ 87	80 (58 – 92)	75 (47 – 91)
AUC (MPV*s)	0.81 (0.65 – 0.96)	≥ 13,700	70 (48 – 85)	83 (55 – 95)

TTU, Time to initial up-slope; Tp, Peak time; TTW, Time to wash-out; MPV, Mean pixel value; PI, Peak intensity; AUC, Area under the curve

<sup>a</sup>Numbers expressed as percentages.

## 4. DISCUSSION

CEUS is an effective and noninvasive method for quantification of pancreatic perfusion as demonstrated in chapters 1 and 2. In this chapter, CEUS was able to detect pancreatic perfusion changes in naturally occurring pancreatitis, as demonstrated by the differing TICs. Measured parameters  $T_p$ , PI and AUC of the pancreas were significantly different from normal controls. Quantification of these parameters enabled differentiation of dogs with pancreatitis from controls. Concurrent secondary duodenal perfusion changes were also observed in the pancreatitis group.

Visually, the pancreas of dogs in the pancreatitis group took a longer time to reach higher PI, and remained contrast-enhanced longer. The duodenum also showed similar patterns of increased echogenicity on CEUS. These visual changes may be subtle in some cases, and assessment depends on subjective impression by the examiner. Therefore, visual assessment is greatly affected by inter-observer variations or presence of bias. Quantifying the perfusion using TIC and measured parameters provides objective analysis to pancreatic perfusion.<sup>11,31</sup>

In the current study, pancreatic perfusion parameters PI and AUC of the pancreatitis group were significantly higher than controls. This was consistent with findings in chapter 2 on cerulein-induced AP in dogs. Additionally,  $T_p$  was also significantly delayed in the pancreatitis group. TTW of the pancreatitis group was also prolonged but was not significant. Perfusion changes were also observed in duodenum of dogs in the pancreatitis group. PI and AUC were significantly increased when compared to controls. This is in contrast with results previously reported in chapter 2, where no perfusion changes secondary to pancreatitis were observed in the duodenum. Perfusion changes seen in this study could be due to the presence

of microcirculatory derangements in the duodenum from local inflammatory effects of pancreatitis, which was not present in experimental pancreatitis (chapter 2) due to the short period of pancreatic insult, but present in naturally occurring pancreatitis.

In particular, measured parameters Tp, PI, and AUC of the pancreas produced the highest AUROC (Table 5). Applying specific cutoff obtained from the ROC curve for Tp enabled detection of pancreatitis with good sensitivity and specificity, while PI and AUC had good sensitivity and specificity, respectively.

As explained in chapter 2, these changes observed in pancreatic perfusion parameters might be associated with microvascular changes seen in the inflamed pancreas.<sup>56</sup> PI was increased due to built-up of MB within obliterated ends of capillaries and slower wash-out of these MB lead to prolonged TTW and increased AUC in this study. Delayed Tp might be associated with the dilated and tortuous capillaries that resulted in more time required for MB to accumulate to PI.

In four dogs, non-enhancing pancreatic parenchymal lesions were identified on CEUS. The enhancement characteristics of these lesions (non-enhancement) on CEUS suggest areas of pancreatic ischemia or necrosis instead of neoplasia such as pancreatic insulinoma (hypo-enhancement or hyper-enhancement) or adenocarcinoma (hypo-enhancement).<sup>25-27,32</sup> However; histopathological confirmation was not available in this study. Although development of pancreatic necrosis reflects poor prognosis in human patients with AP,<sup>32</sup> patient prognosis was good in the present study. All four dogs survived and recovered from pancreatitis with admission into the intensive care unit and appropriate medical therapy. A recent study on CEUS of dogs with AP also reported good prognosis in patients with non-enhancing pancreatic lesions.<sup>34</sup> This could be due to recruitment of patients with milder forms of pancreatitis in the present study, or differences in the disease process between humans and dogs.

Perfusion change of the duodenum secondary to pancreatitis was also investigated in this study. As demonstrated in chapter 1 (study of CEUS of normal dogs), the PI of the pancreas and duodenum was almost equal. In contrast with results from chapter 2 (experimentally induced AP), where no secondary CEUS changes were detected in the duodenum, perfusion changes were detected in this study. Since both organs were more intensely enhanced in dogs with pancreatitis, real-time visual comparison during CEUS examination was not feasible. Therefore, quantitative analysis of duodenal enhancement on CEUS, and subsequent comparison with control group should be performed for objective comparison. In cases where perfusion of the pancreatic parenchyma and duodenum increase concurrently, without presence of primary gastrointestinal disease, suspicion of pancreatitis should also increase.

CEUS was possible in 20/23 (87%) dogs in this study and can be performed relatively easily following B-mode US exam. However, in this study CEUS images were not satisfactory in three dogs. One dog was uncooperative midway during CEUS exam and excessive patient movement was encountered. In another dog, duodenal gas obscured pancreatic imaging during CEUS. In the last dog, overall poor enhancement of abdominal organs were observed, resulting in images that were of insufficient quality for analysis.

A few limitations were present in this study. Firstly, this sample was derived from a single institution resulting in a small sample size. Secondly, dogs enrolled into this study comprised mainly of small- to medium-sized dogs, which differed from the control group. This limitation was due to overrepresentation of small- to medium-sized dogs among Japanese pet-owners, or that smaller dogs are more likely to develop pancreatitis. Additionally, dogs in the pancreatitis group were significantly older than the control group. Although differences in size and age can influence perfusion of the pancreas, the changes observed in the pancreatitis group in this study were paradoxical to perfusion pattern changes

in older patients and smaller-sized dogs. Pancreatic perfusion decreases with age in people, while smaller-sized dogs typically show faster  $T_p$  than medium-sized dogs.<sup>20,72</sup> Thus, the perfusion changes seen in this study could be due to the underlying pancreatic pathology. Thirdly was the lack of histopathology for the definitive diagnosis or classification of pancreatitis. Histopathology to rule out mild enteropathy that could have influenced duodenal perfusion was also lacking. Although only dogs with acute onset of clinical signs were enrolled into this study, differentiation of dogs with acute, chronic or acute-on-chronic pancreatitis cannot be made based on clinical signs.<sup>4,5</sup> The possible mixture of these cases may be the reason why there was an overlap in some the measured parameters and the differences were not as clear as demonstrated in chapter 2. In the previous chapter, perfusion changes were observed on CEUS acutely after pancreatic insult and returned to baseline values with time. In this chapter, because patients were presented to the hospital at various times after first showing clinical signs, CEUS was inevitably performed at different stages of pancreatic inflammation. Fourthly, clinicians on these cases had different levels of experience, resulting in varying abilities to visualize the pancreas on US, as well as ruling out presence of other diseases contributing to clinical signs and biochemical changes. Fifth was the lack of Spec cPL results in control dogs to rule out presence of mild or subclinical pancreatitis. Nevertheless, dogs were clinically healthy and did not show any clinical signs suggestive of pancreatitis before or after CEUS studies were carried out.

Additional research with histological diagnosis and classification of types of pancreatitis is warranted, however this is always difficult in clinical settings where biopsy samples are often not obtained. CEUS may also be potentially useful in monitoring disease progression; therefore future research should include comparison of pancreatic perfusion before and after treatment. It is also important to investigate how well CEUS can differentiate dogs with similar clinical signs but with nonpancreatic disease from dogs with pancreatitis.

Further study is also needed to clarify superiority of CEUS to conventional B-mode US in the diagnosis of canine pancreatitis, especially in cases where abnormal pancreatic lipase immunoreactivity is present, but pancreatic appearance on B-mode US is insignificant.

In conclusion, CEUS can be used in the dog for detecting pancreatic perfusion changes as a possible sign of pancreatic inflammation in naturally occurring pancreatitis. Naturally occurring pancreatitis was characterized by a delayed increase to PI and prolonged hyperechoic enhancement on CEUS. Quantifying the pancreatic perfusion parameters can provide objective and valuable information in differentiating dogs with pancreatitis from normal dogs. When secondary perfusion changes occur concurrently in the duodenum, without primary gastrointestinal disease, suspicion for presence of pancreatitis should increase. Quantitative CEUS may be useful as a noninvasive diagnostic tool in the diagnosis of naturally occurring pancreatitis in dogs.

## 5. SUMMARY

In this chapter, feasibility of using quantitative CEUS to detect pancreatic and duodenal perfusion changes in naturally occurring pancreatitis in dogs was investigated. Differences in perfusion parameters were present between pancreatitis and control group. For the pancreas,  $T_p$  of the pancreatitis group was significantly prolonged when compared to control group.  $TTW$  was also prolonged but was not significant.  $PI$  and  $AUC$  were increased significantly when compared to control group. For the duodenum,  $PI$  and  $AUC$  were significantly increased in pancreatitis group when compared to control group. CEUS can detect pancreatic perfusion changes in naturally occurring pancreatitis and may be useful as a noninvasive diagnostic tool. Naturally occurring pancreatitis was characterized by delayed peak with prolonged hyperechoic enhancement of the pancreas on CEUS. Additionally, duodenal perfusion changes secondary to pancreatitis were also observed.

## GENERAL CONCLUSION

The goal of this study was to determine the feasibility of using quantitative CEUS in the diagnosis of canine pancreatic disease, in particular pancreatitis. The findings of the present study suggest that quantitative CEUS can be used to image the canine pancreas and is useful in detecting pancreatic perfusion changes as a possible sign of pancreatic inflammation. The findings were consistent in experimentally induced pancreatitis, as well as naturally occurring pancreatitis in dogs.

In chapter 1, I have characterized the image enhancement of the normal canine pancreas using two methods of MB administration (bolus injection and continuous infusion). I have also assessed if continuous infusion method can prolong the duration of pancreatic enhancement over that with bolus injection. The contrast-enhancement of the pancreas was characterized by a fast wash-in to an intense peak, and followed by rapid wash-out, when given by bolus injection. With continuous infusion, contrast wash-in to PI was gradual, followed by long plateau and slow wash-out. Median contrast-enhancement duration of the pancreas was significantly prolonged by continuous infusion. Thus, I was able to demonstrate that CEUS could be used to image the canine pancreas, and that prolonged continuous imaging was made possible by the continuous infusion method.

In chapter 2, I have investigated the feasibility of using quantitative CEUS to detect pancreatic perfusional changes in cerulein-induced AP in dogs and to describe the patterns of change over time. Briefly, six dogs were infused with saline and cerulein, at 2 weeks apart, and CEUS of the pancreas and duodenum were performed before, and at 2, 4, 6, and 12 hours after each infusion. Pancreatic perfusion after induction of AP with cerulein was compared to saline controls (before and after saline infusion) as well as before cerulein infusion. In cerulein-induced AP, pancreatic PI increased at 2 and 4 hours when compared to 0 hour, and

at 2, 4, and, 6 hours when compared to control. AUC increased at 4 hours when compared to 0 hour, and at 2 and 4 hours when compared to control. TTW was prolonged at 4 hours when compared to control. No perfusion changes were seen in the duodenum. Thus, I was able to demonstrate feasibility of CEUS in detecting pancreatic perfusion changes in the experimental form of pancreatitis. In particular, intensity parameters PI and AUC can provide useful information in differentiating AP from normal pancreas. Cerulein-induced AP was characterized by prolonged hyperechoic enhancement on CEUS.

In chapter 3, I have investigated the feasibility of using quantitative CEUS to detect pancreatic and secondary duodenal perfusion changes in naturally occurring pancreatitis. Between September 2011 and December 2013, dogs presented to Hokkaido University Veterinary Teaching Hospital and diagnosed with pancreatitis were prospectively enrolled. CEUS of the pancreas and duodenum were performed and measured parameters were compared to normal controls. Differences in perfusion parameters were present between pancreatitis and control group. For the pancreas, Tp of the pancreatitis group was significantly prolonged when compared to control group. TTW was also prolonged but was not significant. PI and AUC were increased significantly when compared to control group. For the duodenum, PI and AUC were significantly increased in pancreatitis group when compared to control group. CEUS can detect pancreatic perfusion changes in naturally occurring pancreatitis and may be useful as a noninvasive diagnostic tool. Naturally occurring pancreatitis was characterized by delayed peak with prolonged hyperechoic enhancement of the pancreas on CEUS. Additionally, duodenal perfusion changes secondary to pancreatitis were also observed.

Future study plans should include a bigger population, with multiple institution involvement for validation of these CEUS data. Additional research with histological diagnosis and classification of types of pancreatitis is also needed. Apart from that, CEUS

may also be potentially useful in monitoring disease progression; therefore future research should include comparison of pancreatic perfusion before and after treatment. It is also important to investigate how well CEUS can differentiate dogs with similar clinical signs but with nonpancreatic disease from dogs with pancreatitis. Further study is also needed to clarify superiority of CEUS to conventional B-mode US in the diagnosis of canine pancreatitis.

In conclusion, through this study I was able to establish a suitable CEUS protocol for pancreatic imaging and have characterized normal CEUS findings in the canine pancreas. CEUS was able to detect pancreatic perfusion changes both in experimentally induced and naturally occurring pancreatitis with high sensitivity and specificity. CEUS is potentially useful as a new diagnostic tool in diagnosing naturally occurring pancreatitis in dogs.

## JAPANESE SUMMARY (要旨)

### Application of contrast-enhanced ultrasonography in diagnosis of canine pancreatic disease

(犬の膵疾患の診断における造影超音波検査の応用)

急性膵炎は犬の膵疾患の中で最も多く極めて重要な疾患であるが、非侵襲的に正確な診断を下すことはしばしば困難である。超音波検査は急性膵炎の診断に有用であるが、膵臓に異常が認められなくても膵炎の存在を否定することはできない。超音波造影剤ソナゾイドを使用した造影超音波検査 (CEUS) は、近年の超音波診断に飛躍的な進歩をもたらした。CEUS における造影増強効果は組織灌流と良好に相関するため、組織内の微小血管の灌流状態をリアルタイムに評価することが可能となった。本研究では、CEUS による定量的評価が犬の膵疾患、特に急性膵炎の診断に有用であるかどうかを検討するため、3 段階の実験を計画した。

第 1 に、まず超音波造影剤を急速投与、または定速持続投与の 2 通りの方法で注入し、健常犬の膵臓がどのように造影増強されるかを検討した。また急速投与方法に比べて定速持続投与方法が造影持続時間を延長させるかについても併せて検討した。8 頭の健常犬を用いて膵臓 CEUS を実施し、時間-エコー輝度曲線 (TIC) を作成した。統計解析を行うため、上昇開始時間 (TTU)、最高点到達時間 (Tp)、エコー輝度低下時間 (TTW)、最高値 (PI) の 4 種の測定項目を設定した。急速投与

した場合、膵臓のエコー輝度は急速に PI まで上昇し、その後急速に低下した。一方、持続投与した場合、膵臓のエコー輝度は徐々に PI まで上昇し、続いて長いプラトーが認められた後に徐々に低下した。膵臓の造影時間の中央値は、持続投与で有意に延長していた。以上の結果から、CEUS は犬の膵臓描出にも適応可能であり、造影剤の持続投与によってより長時間の描出が可能であることが示された。

第 2 に、セルレイン誘発性急性膵炎モデル犬を作出し、急性膵炎における組織灌流の変化を CEUS によって検出可能であるか検討した。またモデル犬における CEUS 所見の経時的な変化についても併せて検討した。健常犬 6 頭に、生理食塩水で希釈したセルレインを  $7.5 \mu\text{g}/\text{kg}/\text{h}$  の投与速度で 2 時間静脈内投与し急性膵炎を誘発した。CEUS は膵炎誘発前 (0 時間)、セルレイン投与の 2 時間後、4 時間後、6 時間後および 12 時間後に実施した。膵臓および十二指腸に関心領域を設定し、TIC を作成した。統計解析のため、TTU、Tp、TTW、PI、曲線下面積 (AUC) の 5 種の測定項目を設けた。またセルレイン誘発性急性膵炎モデル作出の 2 週間前に、全ての健常犬に対し生理食塩水のみを 2 時間かけて投与した後に同様の検討を行い、これを対照群とした。急性膵炎モデル犬の PI は、誘発前に比べ 2 時間後、4 時間後で有意に上昇しており、対照群との比較では 2 時間後、4 時間後、6 時間後に上昇を認めた。AUC は誘発前と比べ 4 時間後で有意に上昇しており、対照群との比較では 2 時間後、4 時間後に上昇を認めた。また急性膵炎モデル犬の TTW は、対照群に比べ 4 時間後に有意な延長が認められた。十二指腸では、組織灌流の変化は観察されなかった。以上の結果から、実験的に誘発した急性膵炎における組織灌流の変化を CEUS によって検出可能であることが示された。特にエコー輝度の指標である PI お

よび AUC は、急性膵炎の診断に有用である可能性が示唆された。またセルレイン誘発性の急性膵炎では、造影持続時間の延長が特徴的な CEUS 所見であった。

第 3 に、実際の膵炎症例における膵臓や十二指腸の組織灌流の変化を、定量的 CEUS によって検出可能であるか検討した。2011 年 9 月から 2013 年 12 月までの期間に北海道大学附属動物病院に来院し、膵炎と診断された犬 23 頭を研究対象とし、膵臓および十二指腸の CEUS から TTU、Tp、TTW、PI、AUC の値を求め、健常群 (n = 12) の値と比較した。膵臓の CEUS では、膵炎症例の Tp は健常群と比較し有意に延長しており、PI および AUC は有意に上昇していた。十二指腸の CEUS では、膵炎症例の PI および AUC が健常群に比べ有意に上昇していた。以上の結果から、CEUS は膵炎症例における膵臓の組織灌流の変化を検出することができ、非侵襲的で有用な診断法となる可能性が示唆された。膵炎症例では、ピーク到達時間の遅延および膵臓の造影増強効果の延長が特徴的な CEUS 所見であった。

今後の研究課題として、これらの CEUS 所見の有用性を検証するため、さらなる症例の蓄積および多施設での検討が必要である。また組織診断に基づいた膵炎の細分類を行い、組織診断と CEUS 所見の相関性についても解析していきたい。一方、CEUS は膵炎の進行をモニタリングする手段としても活用できる可能性があるため、膵炎の治療前後における組織灌流の変化についても比較したいと考えている。さらに、同様の臨床症状を呈する非膵炎疾患との鑑別に CEUS が有用であるかについて検討するとともに、犬の膵炎の診断において、CEUS が通常の B-mode の US より優れていることを明らかにしていきたい。

本研究によって、犬の膵臓の定量的 CEUS 法が確立され、正常犬における膵臓の CEUS 所見が明らかとなった。また本法は急性膵炎モデル、臨床例ともに膵臓

における組織灌流の変化を検出できることが示された。CEUS は犬の膵炎の新たな診断法として有用である可能性が示唆された。

## REFERENCES

1. Newman SJ, Steiner JM, Woosley K, et al. Histologic assessment and grading of the exocrine pancreas in the dog. *J Vet Diagn Invest* 2006;18:115-118.
2. Watson P. Chronic pancreatitis in dogs. *Top Companion Anim Med* 2012;27:133-139.
3. Mansfield C. Acute pancreatitis in dogs: advances in understanding, diagnostics, and treatment. *Top Companion Anim Med* 2012;27:123-132.
4. Hess RS, Saunders HM, Van Winkle TJ, et al. Clinical, clinicopathologic, radiographic, and ultrasonographic abnormalities in dogs with fatal acute pancreatitis: 70 cases (1986-1995). *J Am Vet Med Assoc* 1998;213:665-670.
5. Bostrom BM, Xenoulis PG, Newman SJ, et al. Chronic pancreatitis in dogs: a retrospective study of clinical, clinicopathological, and histopathological findings in 61 cases. *Vet J* 2013;195:73-79.
6. Xenoulis PG, Steiner JM. Canine and feline pancreatic lipase immunoreactivity. *Vet Clin Pathol* 2012;41:312-324.
7. Nyland TG, Mattoon JS, Herrgesell EJ, Wisner ER. Pancreas. In: Nyland TG, Mattoon JS, eds. *Small Animal Diagnostic Ultrasound*, 2nd ed. Philadelphia, PA: WB Saunders Co; 2002:144-157.
8. Saunders HM. Ultrasonography of the pancreas. *Probl Vet Med* 1991;3:583-603.
9. Correas JM, Bridal L, Lesavre A, et al. Ultrasound contrast agents: properties, principles of action, tolerance, and artifacts. *Eur Radiol* 2001;11:1316-1328.
10. Sontum PC. Physicochemical characteristics of Sonazoid, a new contrast agent for ultrasound imaging. *Ultrasound Med Biol* 2008;34:824-833.
11. Haers H, Saunders JH. Review of clinical characteristics and applications of contrast-enhanced ultrasonography in dogs. *J Am Vet Med Assoc* 2009;234:460-470.

12. Xu HX. Contrast-enhanced ultrasound: The evolving applications. *World J Radiol* 2009;1:15-24.
13. Wei K, Jayaweera AR, Firoozan S, et al. Basis for detection of stenosis using venous administration of microbubbles during myocardial contrast echocardiography: Bolus or continuous infusion? *J Am Coll Cardiol* 1998;32:252-260.
14. Nakamura K, Takagi S, Sasaki N, et al. Contrast-Enhanced Ultrasonography for Characterization of Canine Focal Liver Lesions. *Vet Radiol Ultrasound* 2010;51:79-85.
15. Ziegler LE, O'Brien RT, Waller KR, Zagzebski JA. Quantitative contrast harmonic ultrasound imaging of normal canine liver. *Vet Radiol Ultrasound* 2003;44:451-454.
16. Nakamura K, Sasaki N, Murakami M, et al. Contrast-Enhanced Ultrasonography for Characterization of Focal Splenic Lesions in Dogs. *J Vet Intern Med* 2010;24:1290-1297.
17. Ivancic M, Long F, Seiler GS. Contrast harmonic ultrasonography of splenic masses and associated liver nodules in dogs. *J Am Vet Med Assoc* 2009;234:88-94.
18. Haers H, Daminet S, Smets PMY, et al. Use of quantitative contrast-enhanced ultrasonography to detect diffuse renal changes in Beagles with iatrogenic hypercortisolism. *Am J Vet Res* 2013;74:70-77.
19. Waller KR, O'Brien RT, Zagzebski JA. Quantitative contrast ultrasound analysis of renal perfusion in normal dogs. *Vet Radiol Ultrasound* 2007;48:373-377.
20. Johnson-Neitman JL, O'Brien RT, Wallace JD. Quantitative perfusion analysis of the pancreas and duodenum in healthy dogs by use of contrast-enhanced ultrasonography. *Am J Vet Res* 2012;73:385-392.
21. Jimenez DA, O'Brien RT, Wallace JD, Klocke E. Intraoperative contrast-enhanced ultrasonography of normal canine jejunum. *Vet Radiol Ultrasound* 2011;52:196-200.
22. Pey P, Vignoli M, Haers H, et al. Contrast-enhanced ultrasonography of the normal canine adrenal gland. *Vet Radiol Ultrasound* 2011;52:560-567.

23. Bigliardi E, Ferrari L. Contrast-enhanced ultrasound of the normal canine prostate gland. *Vet Radiol Ultrasound* 2011;52:107-110.
24. Gaschen L, Angelette N, Stout R. Contrast-Enhanced Harmonic Ultrasonography of Medial Iliac Lymph Nodes in Healthy Dogs. *Vet Radiol Ultrasound* 2010;51:634-637.
25. Vanderperren K, Haers H, Van der Vekens E, et al. Description of the use of contrast-enhanced ultrasonography in four dogs with pancreatic tumours. *J Small Anim Pract* 2014;55:164-169.
26. Nakamura K, Lim SY, Ochiai K, et al. Contrast-Enhanced Ultrasonographic Findings in Three Dogs with Pancreatic Insulinoma. *Vet Radiol Ultrasound* 2014; doi: 10.1111/vru.12177.
27. D'Onofrio M, Zamboni G, Faccioli N, et al. Ultrasonography of the pancreas. 4. Contrast-enhanced imaging. *Abdom Imaging* 2007;32:171-181.
28. D'Onofrio M, Zamboni G, Tognolini A, et al. Mass-forming pancreatitis: value of contrast-enhanced ultrasonography. *World J Gastroenterol* 2006;12:4181-4184.
29. Golea A, Badea R, Socaciu M, et al. Quantitative analysis of tissue perfusion using contrast-enhanced transabdominal ultrasound (CEUS) in the evaluation of the severity of acute pancreatitis. *Med Ultrason* 2010;12:198-204.
30. Badea R, Seicean A, Diaconu B, et al. Contrast-enhanced ultrasound of the pancreas- a method beyond its potential or a new diagnostic standard? *J Gastrointestin Liver Dis* 2009;18:237-242.
31. Kersting S, Konopke R, Kersting F, et al. Quantitative perfusion analysis of transabdominal contrast-enhanced ultrasonography of pancreatic masses and carcinomas. *Gastroenterology* 2009;137:1903-1911.
32. Ripolles T, Martinez MJ, Lopez E, et al. Contrast-enhanced ultrasound in the staging of acute pancreatitis. *Eur Radiol* 2010;20:2518-2523.

33. Rickes S, Uhle C, Kahl S, et al. Echo enhanced ultrasound: a new valid initial imaging approach for severe acute pancreatitis. *Gut* 2006;55:74-78.
34. Shanaman MM, Schwarz T, Gal A, O'Brien RT. Comparison between survey radiography, B-mode ultrasonography, contrast-enhanced ultrasonography and contrast-enhanced multi-detector computed tomography findings in dogs with acute abdominal signs. *Vet Radiol Ultrasound* 2013;54:591-604.
35. Gaschen L, Schur D, Kearney M. Contrast harmonic ultrasound imaging of the normal pancreas and pancreatitis in dogs. Proceedings of ACVR Annual Scientific Meeting 2007 Nov 27- Dec 1; Chicago, IL
36. Chan YC, Leung PS. Acute pancreatitis: animal models and recent advances in basic research. *Pancreas* 2007;34:1-14.
37. An L, Li W, Yao KC, et al. Assessment of contrast-enhanced ultrasonography in diagnosis and preoperative localization of insulinoma. *Eur J Radiol* 2011;80:675-680.
38. Nakamura K, Sasaki N, Yoshikawa M, et al. Quantitative Contrast-Enhanced Ultrasonography of Canine Spleen. *Vet Radiol Ultrasound* 2009;50:104-108.
39. König HE, Sautet J, Liebich H-G. Digestive System. In: König HE, Liebich H-G, eds. *Veterinary Anatomy of Domestic Mammals: Textbook and Colour Atlas*, 2nd ed. Stuttgart, Germany: Schattauer GmbH; 2004:340-342.
40. Dominique P. Pancreas. In: Dominique P, d'Anjou MA, eds. *Atlas of Small Animal Ultrasonography*. Oxford: Blackwell Publishing; 2008:319-338.
41. Albrecht T, Urbank A, Mahler M, et al. Prolongation and optimization of Doppler enhancement with a microbubble US contrast agent by using continuous infusion: preliminary experience. *Radiology* 1998;207:339-347.

42. Kuntz-Hehner S, Goenechea J, Pohl C, et al. Continuous-infusion contrast-enhanced US: in vitro studies of infusion techniques with different contrast agents. *Radiology* 2001;220:647-654.
43. Okada M, Hoffmann CW, Wolf KJ, Albrecht T. Bolus versus continuous infusion of microbubble contrast agent for liver US: initial experience. *Radiology* 2005;237:1063-1067.
44. Landmark KE, Johansen PW, Johnson JA, et al. Pharmacokinetics of perfluorobutane following intravenous bolus injection and continuous infusion of sonazoid in healthy volunteers and in patients with reduced pulmonary diffusing capacity. *Ultrasound Med Biol* 2008;34:494-501.
45. Cornell K, Fischer J. Surgery of the exocrine pancreas. In: Slatter D. ed. *Textbook of Small Animal Surgery*. Philadelphia, PA: WB Saunders Co; 2002:752-753.
46. Kanemoto H, Ohno K, Nakashima K, et al. Characterization of canine focal liver lesions with contrast-enhanced ultrasound using a novel contrast agent-sonazoid. *Vet Radiol Ultrasound* 2009;50:188-194.
47. Kutara K, Asano K, Kito A, et al. Contrast harmonic imaging of canine hepatic tumors. *J Vet Med Sci* 2006;68:433-438.
48. Watanabe R, Matsumura M, Chen CJ, et al. Gray-scale liver enhancement with Sonazoid (NC100100), a novel ultrasound contrast agent; detection of hepatic tumors in a rabbit model. *Biol Pharm Bull* 2003;26:1272-1277.
49. Moon ML, Biller DS, Ambrust LJ. Ultrasonographic appearance and etiology of corrugated small intestine. *Vet Radiol Ultrasound* 2003;44:199-203.
50. Cullen JM, Brown DL. Hepatobiliary system and exocrine pancreas. In: Zachary JF, McGavin MD, eds. *Pathologic Basis of Veterinary Disease*, 5th ed. Missouri, MO: Elsevier; 2012:454-457.

51. Renner IG, Wisner JR Jr. Ceruletide-induced acute pancreatitis in the dog and its amelioration by exogenous secretin. *Int J Pancreatol* 1986;1:39-49.
52. Lamb CR, Simpson KW. Ultrasonographic Findings in Cholecystokinin-Induced Pancreatitis in Dogs. *Vet Radiol Ultrasound* 1993;36:139-145.
53. Morita Y, Takiguchi M, Yasuda J, et al. Endoscopic and transcutaneous ultrasonographic findings and grey-scale histogram analysis in dogs with caerulein-induced pancreatitis. *Vet Q* 1998;20:89-92.
54. Hofbauer B, Saluja AK, Lerch MM, et al. Intra-acinar cell activation of trypsinogen during caerulein-induced pancreatitis in rats. *Am J Physiol* 1998;275:G352-362.
55. Simpson KW, Beechey-Newman N, Lamb CR, et al. Cholecystokinin-8 induces edematous pancreatitis in dogs associated with short burst of trypsinogen activation. *Dig Dis Sci* 1995;40:2152-2161.
56. McEntee G, Leahy A, Cottell D, et al. Three-dimensional morphological study of the pancreatic microvasculature in caerulein-induced experimental pancreatitis. *Br J Surg* 1989;76:853-855.
57. Su KH, Cuthbertson C, Christophi C. Review of experimental animal models of acute pancreatitis. *HPB (Oxford)* 2006;8:264-286.
58. Ilkiw JE. Other potentially useful new injectable anesthetic agents. *Vet Clin North Am Small Anim Pract* 1992;22:281-289.
59. Lim SY, Nakamura K, Morishita K, et al. Qualitative and Quantitative Contrast Enhanced Ultrasonography of the Pancreas Using Bolus Injection and Continuous Infusion Methods in Normal Dogs. *J Vet Med Sci* 2013;75:1601-1607.
60. Cosgrove D, Eckersley R. Contrast-Enhanced Ultrasound: Basic Physics and Technology Overview In: Lencioni R, ed. *Enhancing the Role of Ultrasound with Contrast Agents*. Milan, Italy: Springer; 2006:3-14.

61. Gress TM, Arnold R, Adler G. Structural alterations of pancreatic microvasculature in cerulein-induced pancreatitis in the rat. *Res Exp Med (Berl)* 1990;190:401-412.
62. Klar E, Schratt W, Foitzik T, et al. Impact of microcirculatory flow pattern changes on the development of acute edematous and necrotizing pancreatitis in rabbit pancreas. *Dig Dis Sci* 1994;39:2639-2644.
63. Solanki NS, Barreto SG. Fluid therapy in acute pancreatitis. A systematic review of literature. *JOP* 2011;12:205-208.
64. Hall J. Overview of the Circulation; Biophysics of Pressure, Flow, and Resistance. In: Hall J, ed. *Guyton and Hall Textbook of Medical Physiology*, 12th ed. Philadelphia, PA: WB Saunders Co; 2011:157-166.
65. Piironen A. Severe acute pancreatitis: contrast-enhanced CT and MRI features. *Abdom Imaging* 2001;26:225-233.
66. Jaeger JQ, Mattoon JS, Bateman SW, Morandi F. Combined use of ultrasonography and contrast enhanced computed tomography to evaluate acute necrotizing pancreatitis in two dogs. *Vet Radiol Ultrasound* 2003;44:72-79.
67. Tsuji Y, Takahashi N, Tsutomu C. Pancreatic Perfusion CT in Early Stage of Severe Acute Pancreatitis. *Int J Inflam* 2012;2012:497386.
68. Delrue L, Blanckaert P, Mertens D, et al. Tissue perfusion in pathologies of the pancreas: assessment using 128-slice computed tomography. *Abdom Imaging* 2012;37:595-601.
69. Bize PE, Platon A, Becker CD, Poletti PA. Perfusion measurement in acute pancreatitis using dynamic perfusion MDCT. *AJR Am J Roentgenol* 2006;186:114-118.
70. Lim SY, Nakamura K, Morishita K, et al. Qualitative and quantitative contrast-enhanced ultrasonographic assessment of cerulein-induced acute pancreatitis in dogs. *J Vet Intern Med* 2014;28:496-503.

71. DeLong ER, DeLong DM, Clarke-Pearson DL. Comparing the areas under two or more correlated receiver operating characteristic curves: a nonparametric approach. *Biometrics* 1988;44:837-845.
72. Tsushima Y, Kusano S. Age-dependent decline in parenchymal perfusion in the normal human pancreas: measurement by dynamic computed tomography. *Pancreas* 1998;17:148-152.

## ACKNOWLEDGEMENTS

The PhD journey is not one that can be achieved alone. Along the way, countless people have contributed to its contents, supported, and encouraged me.

In all things, I have the Lord to thank. He is my ultimate source of strength and perseverance. I cannot thank Him enough for his gift of education to me.

I wish to thank the person who made it all possible, my supervisor, Dr. Mitsuyoshi Takiguchi (Graduate School of Veterinary Medicine, Hokkaido University) for giving me the opportunities to achieve my goals and aspirations, and for his constant encouragement and guidance. Without him, I would have never learnt and experienced as much as I did.

I wish to also thank Drs. Masahiro Yamasaki (Faculty of Agriculture, Iwate University), Yoshiaki Habara (Graduate School of Veterinary Medicine, Hokkaido University), and Yumiko Kagawa (Graduate School of Veterinary Medicine, Hokkaido University) for their time and effort in providing priceless advice and critical comments into making this thesis a better one.

I am also greatly indebted to my mentor Dr. Kensuke Nakamura (Graduate School of Veterinary Medicine, Hokkaido University), who had taken his time and effort to critically evaluate my research, papers, and presentations. Without his insightful guidance, my work would not have been improved to its current state.

I also wish to thank Drs. Hiroshi Ohta (Graduate School of Veterinary Medicine, Hokkaido University) and Keitaro Morishita (Graduate School of Veterinary Medicine, Hokkaido University) for their constant support and assistance. My gratitude also extends to my wonderful seniors; Drs. Masahiro Murakami and Noboru Sasaki, and my fellow comrades; Drs. Tatsuyuki Osuga and Nozomu Yokoyama for their relentless advice and ideas when I was at my wit's end. I also wish to thank the Laboratory of Internal Medicine of

Hokkaido University for helping me with my experiments and for being my family here in Sapporo.

I am also greatly indebted to Dr. Malaika Watanabe (Faculty of Veterinary Medicine, Universiti Putra Malaysia), for encouraging me to pursue this path. Many thanks also goes to my endearing friends, Dr. Arshana Amin, Sharon Lau, and Tomoko Sasaki for their priceless gift of friendship and strong support throughout my stay in Sapporo. I also thank my church and its members for always including me into their prayers.

My utmost gratitude goes to my family, who has been my constant source of love and support and to my friends in Malaysia who have kept in contact despite the distance.

Last but not least, to Lukas Leong, who has been my biggest cheerleader throughout this journey.